Fingerprint Alteration Detection

John H. Ellingsgaard

Kongens Lyngby 2013
IMM-M.Sc.-2013-41

Technical University of Denmark
Department of Applied Mathematics and Computer Science
Building 303B, DK-2800 Kongens Lyngby, Denmark
Phone +45 45453031
compute@compute.dtu.dk
www.imm.dtu.dk IMM-M.Sc.-2013-41

Summary (English)

Fingerprint alteration is the procedure of attempting to change or remove characteristics of ones fingerprint in order to avoid identification. Alterations can be performed to the fingertips by various means, such as scraping, cutting, burning or transplanting skin. Unnatural fingerprint patterns are commonly introduced in altered fingerprints.

The goal of the thesis is to propose a method to detect if a fingerprint has been altered or not.

The thesis includes a study on the characteristics of altered fingerprints and on the current state-of-the-art alteration detection algorithm. The proposed method will take a localised approach analysing attributes and characteristics of local areas of the fingerprint in order to identify discrepancies and irregularities.

Preface

This thesis was prepared at the department of Informatics and Mathematical Modelling at the Technical University of Denmark in cooperation with the Norwegian Biometrics Laboratory in fulfilment of the requirements for acquiring an M.Sc. in Informatics.

The thesis deals with the problem of fingerprint alteration. An approach for detecting altered fingerprints is proposed and evaluated.

The thesis consists of 10 chapters and appendixes which give a detailed description of the proposed alteration detection method together with the initial experimental results.

Lyngby, 30-June-2013

John H. Ellingsgaard

Acknowledgements

Firstly, I would like to thank Prof. Dr. Christoph Busch for giving me the opportunity to join the biometric research team at the Norwegian Information Security Laboratory in Gjøvik. I am very grateful for the interest and support given throughout the research period which has been far greater than I would ever have imagined.

I would also like to thank Ctirad Sousedik for supervising my project. His invaluable advice, support and encouragement has been the foundation for the successful achievement of this project. Thank you for sharing your knowledge and taking so much time out of your already busy schedule to guide me in the right directions.

I want to express my gratitude to Prof. Rasmus Larsen for supervising my project at the Technical University of Denmark.

Contents

Chapter 1

Introduction

Flow-like patterns of ridges and valleys exists on the surface of the palms and soles. Researchers have shown that these ridges, called friction ridges, improve tactile sensitivity [SLPD09] and probably also assist in improving the grip of objects in moist conditions and even allow the skin to stretch more easily [WE09].

Apart from these biological benefits and features that aid the skin, friction ridges also contain biometric characteristics and play an important part in biometric recognition. This is down to the fact that the pattern of friction ridges on each finger is unique and immutable [JFNeb]. Even identical twins can be distinguished based on their fingerprints [JPP02], even though they do actually share similarities [JPP01].

Identification using fingerprints is probably the most matured and widespread biometric technique that currently exists. Fingerprints have a long history as a tool for identification and forensic purposes [Int05]. Technological advancement has lead to the development of so-called Automated Fingerprint Identification Systems (AFISs) which are primarily used by border control and law enforcement agencies for identification purposes.

One such application is the Visa Information System (VIS) which enables Schengen states to exchange visa data. The system is based on a centralised architecture. The system consists of distributed national interfaces (NI-VIS) that

are linked together with a central information system (CS-VIS) [Com12]. The system contains alphanumeric data as well as biometric data in the form of fingerprints and photographs, for identification and verification purposes.

Some of the purposes of VIS is to prevent *visa shopping* and facilitating the fight against fraud. However, another purpose of a border control biometrics system is to identify individuals on a watch list [Com10]. One method used to avoid identification of such a system is to alter one's fingerprints e.g. by obfuscating ridge flows by scraping, cutting or burning, or even in extreme measures using plastic surgery [YFJ12].

The use of fake fingers or prints are also of great concern. Extensive research has been done on detecting fake fingers yielding techniques such as perspiration checks [AS09], analysing skin distortion [ACMM06] and even analysing odour using *electronic noses* [BFMM05]. Unfortunately, many of the most reliable techniques require expensive equipment which in some cases lead to requirements of additional policies using rudimentary methods, e.g. in Germany border control officers are required to look on the fingerprint scanner and on the fingers of the visa holder in order to detect fake fingers [SRBG11].

Altered fingerprints on a real finger are not necessarily easy to spot by a quick glance on the fingers of a person. Changes can be subtle to the naked eye and would require officers to do a closer inspection of every finger to positively identify alterations.

Fake fingers are typically used to impersonate and take on another persons identity, while altered fingerprints are typically to conceal ones identity in order to avoid identification.

The international standardisation project ISO/IEC 30107 [ISO12] defines the Attack Presentation Characteristic (APC) which is the characteristic presented in a sensor-based attack. Artificial (fake) or human-based characteristics are the two main categories; a third category covering natural cases such as animal- and plant-based APCs is also included for completeness.

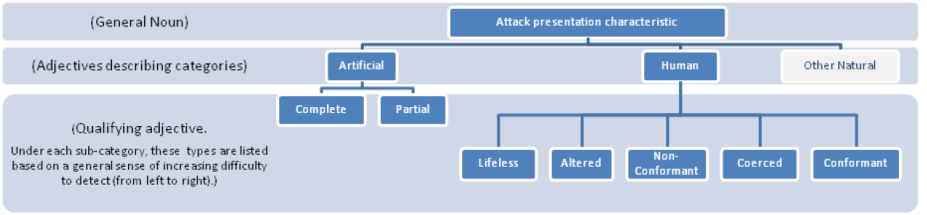

Figure 1.1: Types of presentation attacks. Source: [ISO12].

The two main categories have further subcategories of characteristics. Figure 1.1 gives an overview of the types of presentation attacks while examples of each of the characteristics belonging to the two main categories are shown in Table 1.1.

Main	Characteristic	Example
Artificial	Complete	gummy finger
	Partial	glue on finger
Human	Lifeless	cadaver part, severed finger/hand
	Altered	mutilation, surgical switching of fingerprints
	Non-Conformant	tip or side of finger
	Coerced	unconscious, under duress
	Conformant	zero effort impostor attempt

Table 1.1: Artificial and human attack presentation characteristics [ISO12].

This project will deal with the aspect of detecting altered fingerprints. More precisely, according to the aforementioned standard, the project concentrates on *altered, human, attack-presentation characteristics*. The goal of this project is not to identify the actual identity of an individual that has altered fingerprints, but instead to detect and raise an alarm if a fingerprint is considered to be altered.

This thesis can be structurally divided into four parts. The first part introduces some characteristics of altered fingerprints. The second part describes a chosen state-of-the-art algorithm for detecting altered fingerprints. The third part part is the contribution of a proposed algorithm for detecting altered fingerprints. Finally the results are evaluated and discussed.

Chapter 2

Altered Fingerprints

This chapter will describe some of the characteristics of altered fingerprints. More specifically, it will categorise the fingerprints into three common categories; the characteristics of each category will then be explored and analysed.

2.1 History

Fingerprints have a long history of being used for forensics and other identification purposes. As the importance of the usage of fingerprints has grown through time and identification techniques have improved, the instances of individuals trying to deceive the system and avoid being identified have become more common. Already back in 1935 H. Cummins [Cum35] published information on three criminal cases involving altered fingerprints. The cases were the following:

- John Dillinger applied acid to the finger tips in order to burn and permanently change the fingerprints. After his death it was determined that careful examination of the remaining undamaged areas of the fingerprints would be enough to positively identify him solely on the fingerprints.
- Gus Winkler mutilated four of his fingerprints on the left hand, excluding the thumb, possibly by the combination of slashing and deeply scraping.

He was actually successful in changing his pattern type from double loop to left loop (see Figure 2.1).

- Jack Klutas unsuccessfully tried to evade identification by slashing his finger tips.

(a) Before mutilation **(b)** After mutilation

Figure 2.1: Gus Winkler succeeded in changing the pattern type from double loop to left loop. Source: [Cum35].

The aforementioned incidents were all observed on hardened criminals and gangsters where authorities were successful in identifying all three sets of fingerprints. Other incidents demonstrate individuals using more advanced and inventive techniques for masquerading their identity and baffling officials:

- Robert J. Philipps (1941) attempted to completely erase his fingerprints by transplanting skin grafted from the side of his chest onto the fingertips [HC43].
- Jose Izquierdo (1997) cut a "Z" shaped cut (see Figure 2.2) on his fingertip and exchanged the two flaps of skin. After manually reconstructing his real fingerprint images officials managed to reveal his true identity; this came with a large cost of approximately 170 hours of manual and computer searching [Wer98].
- Donald Roquierre cut circles in the middle of each finger, removed the resulting skin (deep down to include the basal layer of skin where fingerprints form), turned the circles upside down and replaced them on different fingers. He sewed them on with a needle and thread [Wer93].

The above mentioned examples are actual criminal cases. However, border crossings are seeing an increased amount of asylum seekers and migrants with

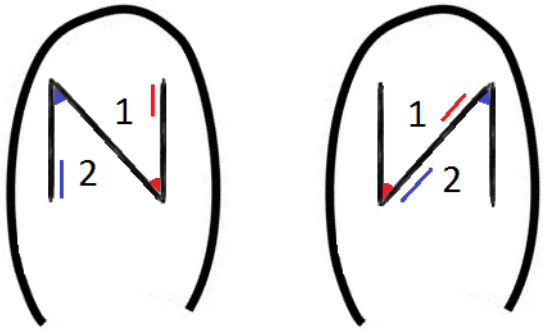

(a) Before z-cut **(b)** After z-cut

Figure 2.2: Illustrations of how two flaps of skin can be exchanges within a "Z" shaped cut. The numbers and colours are merely for illustration purposes to show skin positions before and after the surgery.

mutilated fingerprints who try to avoid being identified.

- In 2009 a Chinese woman successfully evaded identification when entering Japan by using plastic surgery to swap the fingerprints from her right and left hand. She was only discovered when arrested on separate charges and police noticed that her fingers had unnatural scars [New09].

- The MailOnline reported that it is common that migrants wanting to enter Britain through Calais mutilate their fingertips to hide their identity [Mai09].

Images that show actual fingers with altered fingertips can be seen in Figure 2.3.

2.2 Characteristics

Based on the observations by Feng, J. *et al* [FJR09] altered fingerprints are classified into three categories based on the changes in ridge pattern due to alteration [YFJ12]. The classification types are based on the fingerprint image and not on the actual alteration process[YFJR09].

(a) Skin transplanted from sole of foot

(b) Bitten fingertips

Figure 2.3: Images of altered fingertips. Source: [JY12].

The following sections will describe the characteristics of fingerprints in each of these categories. Analysing discrepancies and special features of fingerprints in these subcategories will firstly serve as the basis for understanding the structure of common alterations.

2.2.1 Obliteration

Probably the most common form of alteration is *obliteration*. The word obliteration basically means to destroy, remove or erase. Obliteration is the means of diminishing the quality of the friction ridge patterns on the fingertips in order to make it problematic (or even impossible) to match with the original.

Obliteration can be performed by incision, scraping, burning, applying acids or transplanting smooth skin [FJR09]. The previous section has several examples of obliteration, e.g. Jack Klutas used incision, John Dillinger mutilated his fingertips with acids and Robert J. Philipps transplanted skin from the sides of his chest to his fingertips.

Obliteration can be perceived as a natural extension to the problem of identifying low quality fingerprints. The quality of unaltered fingerprints can vary depending on different factors such as the quality of the actual scan or damages such as ridges broken by flexion creases or scars. Also skin diseases such as eczema or warts can have a degrading impact on the quality of the friction ridge patterns (see Figure 2.4).

(a) Finger eczema

(b) Wart

(c) Finger eczema

(d) Wart

Figure 2.4: Diseases can obliterate a fingerprint. Images and subsequent fingerprint images do not belong to the same subjects. Source: [DDU13]

Good quality friction ridge patterns in an obliterated fingerprint image are the actual unaltered ridge patterns. Therefore, If a large enough area of the fingerprint is undamaged it can hold enough information for an automatic fingerprint information system to positively match it to the original fingerprint image. Therefore successful identification is heavily dependant upon the quality level of the fingerprint.

Fingerprint quality assessment software such as NIST Fingerprint Image Quality (NFIQ) could in many cases be used to deny enrolling or comparing a heavily obliterated fingerprint, since the quality would simply be deemed too low for comparison.

Obliteration	
Definition	destroy, remove or erase.
Performed by	incision, scraping, burning, applying acids or transplanting smooth skin.
Characteristics	areas of low quality friction ridge patterns.

Table 2.1: Characteristics of obliteration.

2.2.2 Distortion

Distortion is the reshaping of the original patterns of the friction ridges. This can be done by removing and reorganising portions of skin from fingertips or by transplanting other skin with friction ridge patterns unto the fingertip. The resulting fingerprints on the fingertips will have unnatural ridge patterns.

Previously it was described how Jose Izquierdo distorted his fingerprints by exchanging two portions of skin on the fingertip by a "Z" shaped cut. Figure 2.5 shows the actual fingerprint images of Jose Izquierdo.

(a) Before z-cut **(b)** After z-cut

Figure 2.5: Jose Izquierdo altered his fingerprints by exchanging two portions of skin using a "Z" shaped cut. Source: [Wer98].

Fingertips that have been successfully distorted will have a high quality level, since they will have clearly visible friction ridge patterns throughout the whole fingerprints; possibly even preserving ridge properties such as width and frequency over the entire fingerprint area.

A closer look at a distorted fingerprint will however show clear irregularities. There will typically be sudden changes in the orientation of friction ridges along the scars where different skin patches are joined together. Also, distortion can result in unnatural distribution of singular points.

Distortion	
Definition	misrepresentation, misshape, a change in perception so that it does not correspond to reality (psychology).
Performed by	removing and reorganising portions of skin from fingertips or by transplanting skin with friction ridge patterns.
Characteristics	unnatural ridge patterns and scarred areas.

Table 2.2: Characteristics of distortion.

Unaltered fingerprints normally have a flowing and smooth orientation field throughout the whole fingerprint except in singular points.

2.2.3 Imitation

The most advanced category of altered fingerprints are imitated fingerprints. This is not referring to spoofing or false fingers but instead to the quality of alteration.

Imitated fingerprints have friction ridge patterns that both preserve ridge properties, e.g. width and frequency, while also containing the typical smooth orientation field pattern found in unaltered fingertips.

A typical imitation technique includes transplantation of a large area of friction ridge skin. An example of such a transplantation is the Chinese woman, described earlier, who evaded identification by swapping her left and right fingerprints using plastic surgery. Another technique is simply to remove a portion of friction ridge skin and thereafter join together the remaining skin. For this to be a success, friction ridges on each side of the scar must principally avoid abrupt changes in orientations. Gus Winkler was successful in this technique, even changing the type of his finger pattern in the process.

The main difference between *distortion* and *imitation* is the fact that imitated fingerprints maintain the smooth orientation field characteristics of an unaltered fingerprint.

The problem with imitated fingerprints is that they contain so many properties of an unaltered fingerprint and in such a good quality that it will successfully pass fingerprint quality assessment software. Well executed imitation can even

Imitation	
Definition	copy, mimic or appear like.
Performed by	transplanting large areas of skin with friction ridge patterns or careful incision and reshaping.
Characteristics	natural ridge patterns.

Table 2.3: Characteristics of imitation.

be hard to spot even with a close inspection of the fingertips by the naked eye.

2.2.4 Focus of Thesis

The main focus of this thesis will be on distorted fingerprints. The main reasons for the decision are the following:

- Obliterated fingerprints will, in most cases, already be processed correctly based on the area and amount of obliteration. Either fingerprint quality assessment software will evaluate that the fingerprint quality is too low or it will be processed correctly in the biometric identification system.
- Distorted fingerprints can have a high quality level and share many properties with unaltered fingerprints. However, they have clearly identifiable properties, such as irregular and abrupt changes in the orientation of friction ridges.
- Imitated fingerprints share too many properties with unaltered fingerprints, such as a natural ridge flow throughout the whole fingerprint and natural distribution of minutia and singular points. It is assumed that it is virtually impossible to identify that good quality imitation is an altered finger.

Chapter 3

Alteration Detection Algorithms

Relatively limited research, with significant and proven results, has been done in the field of automatically detecting altered fingerprints.

Yoon *et al*[YFJ12] proposed a very successful technique based on analysing discontinuity and abnormality in the flow of the friction ridges along with analysing the spatial distribution of minutiae.

This section will describe the construction of the state-of-the-art algorithm. This algorithm will serve as the basis for further research into the topic of identifying altered fingerprints.

3.1 Algorithm Overview

The algorithm is based on two different analyses:

- Analysis of the friction ridge orientations. Fingerprints generally have a smooth ridge flow except near singular points. Altered fingerprints will

typically result in irregular and abrupt changes in the ridge flow in some areas of the fingerprint. This approach tries to identify regions of unnatural ridge flow. This specific analysis will be called Orientation Field Analysis (OFA) in this thesis.

- Analysis of minutiae distribution. A minutia point is located at local discontinuities in the fingerprint pattern where friction ridges begin, terminate or bifurcate. The analysis will be named Minutia Distribution Analysis (MDA).

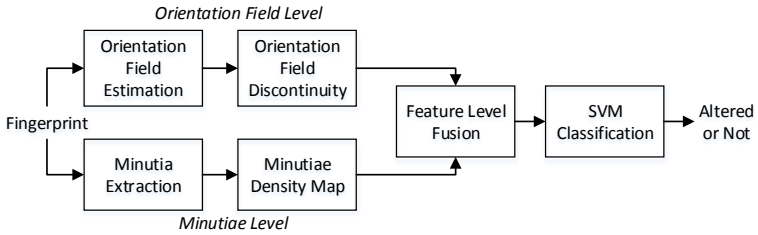

Figure 3.1: Flowchart of the algorithm. Source: [YFJ12]

Feature vectors are constructed from each of the analyses, fused into one larger feature vector and fed into a Support Vector Machine (SVM) for classification. Figure 3.1 shows a flowchart of the alteration detection algorithm.

The following sections will describe the two analyses used in the algorithm and how the feature vectors are constructed.

3.2 Orientation Field Analysis

The OFA uses a mathematical model for constructing an approximation of an estimated ridge flow of the fingerprint. The analysis identifies discontinuities based on differences of the ridge flow approximation and estimation, e.g. areas where the approximation is unable to correctly simulate the actual fingerprint image.

The orientation of friction ridges, typically called *orientation field* and denoted θ, is defined as an image where $\theta(x, y)$ holds the estimated orientation at pixel (x, y).

The steps of the analysis are the following:

1. Normalisation. Formats the fingerprint image to have a common rotation and size.
2. Segmentation. The foreground of the fingerprint is separated from the background of the image in order to be able to only analyse the actual fingerprint. Segmentation is not described further in this section. See section 5.2 for a detailed description of segmentation.
3. Orientation field estimation. The $n \times n$ block-wise averaged orientation field, $\theta(x, y)$, is computed using the gradient-based method. A typical block size used in this work is 8×8.
4. Orientation field approximation. A polynomial model is used to approximate the orientation field $\theta(x, y)$ to obtain $\hat{\theta}(x, y)$.
5. Orientation error map. The absolute difference between the orientation field $\theta(x, y)$ and the approximation $\hat{\theta}(x, y)$ is computed to yield an error map, $\epsilon(x, y)$.

The steps will be described a little closer below. Since the orientation field serves as a central part of this method and also in the upcoming proposed algorithm, a technique for constructing such an orientation field will be described in more detail.

3.2.1 Normalisation

In image processing, the term *normalisation* typically is a process of modifying the range of pixel intensity values. Here, it deals with adapting a common alignment and size of the fingerprint image to ensure invariance with respect to translation and rotation.

A rectangular region of the fingerprint is located, rotated to be aligned along the longitudinal direction, and cropped using the fingerprint segmentation algorithm of the NIST Biometric Image Software (NBIS) [WGTW12]. The cropped image is resized to 512×480 pixels.

3.2.2 Orientation Field Estimation

The orientation flow of the friction ridges is a global feature of fingerprints that is very important in AFIS. The *orientation field* is the local orientation of the friction ridges. It serves as an essential part in all stages of analysing a

fingerprint, such as preprocessing and feature extraction. The orientation field will be used in several of the upcoming analyses.

An orientation image represents an intrinsic property of the fingerprint image and defines invariant coordinates for ridges and valleys in a local neighbourhood [LHJ98a]. The orientation field basically holds information on the local orientations of friction ridges. Orientations are typically defined in the range $[0, \pi)$.

Depending on the context, this thesis uses both pixel-wise and block-wise orientation fields. Pixel-wise orientation is the estimated orientation of each pixel. Instead of using local ridge orientation at each pixel, it is common to partition the image into smaller blocks. The block-wise orientations are derived by simply averaging the orientations within each block. Figure 3.2 shows the orientation field of two fingerprint images; the pixel-wise orientations are illustrated in greyscale while block-wise orientations use lines to represent orientations within each block.

There are two common approaches to compute the orientation field of a fingerprint: filter-bank based approaches and gradient-based approaches. An example of a filter-bank based approach is a method proposed by Kamei and Mizoguchi [KM95] using directional filters in the frequency domain. According to Gu and Zhou [GZ03] filter-bank based approaches are more resistant to noise than gradient-based approaches, but computationally expensive.

Gradient-based methods seems to be the most common approach for extracting local ridge orientation; probably since it is the *simplest and most natural approach* [MMJP09]. This thesis will adopt a gradient-based approach.

3.2.2.1 Pixel Orientation

A natural approach for extracting ridge orientation is based on computation of gradients in the fingerprint image. The first step is determining the gradient components δ_x and δ_y for each pixel in the image. This implementation uses a *Sobel* operator to define the pixel gradient components. The Sobel operator is a discrete differentiation operator that computes an approximation of the gradient of the image intensity.

The Sobel operator uses two 3 x 3 gradient filters - one for calculating the horizontal changes in the image and the other for vertical changes. The two kernels are illustrated in Figure 3.3 where S_x is the kernel for the horizontal direction and S_y is the vertical.

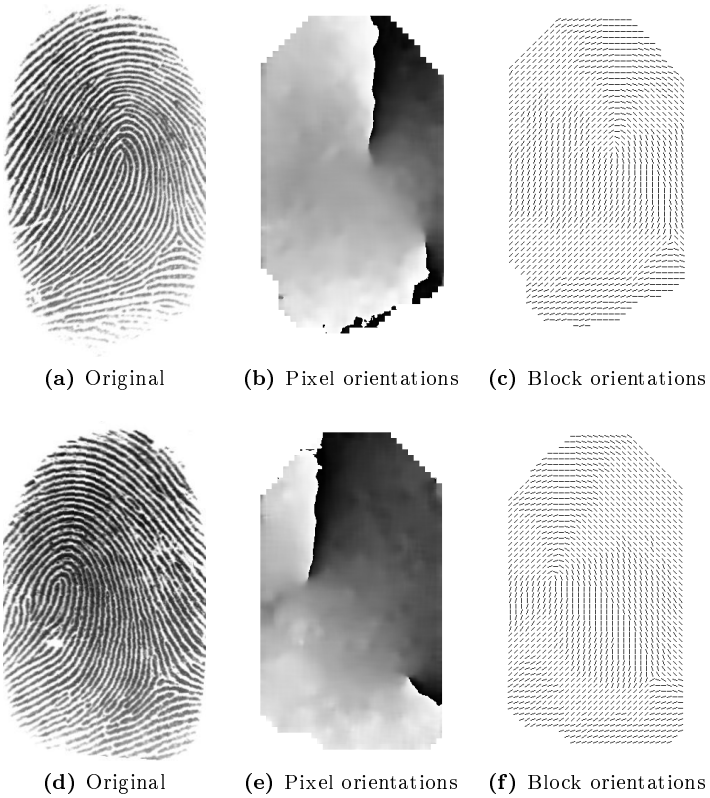

(a) Original **(b)** Pixel orientations **(c)** Block orientations

(d) Original **(e)** Pixel orientations **(f)** Block orientations

Figure 3.2: Orientation of fingerprints. (a) (d) show the original fingerprint images (Source: [CMM+04]), (b) (e) contain pixel-wise orientations in gray-scale, and (c) (f) show block-wise orientations.

For each pixel, (i, j), in the image two two-dimensional convolutions with the Sobel kernels are computed, yielding the gradient components $\delta_x(i, j)$ and $\delta_y(i, j)$. Note that border pixels do not have their gradients calculated as they don't have neighbouring pixels in every direction.

$$S_y = \begin{bmatrix} -1 & -2 & -1 \\ 0 & 0 & 0 \\ 1 & 2 & 1 \end{bmatrix} \qquad S_x = \begin{bmatrix} -1 & 0 & 1 \\ -2 & 0 & 2 \\ -1 & 0 & 1 \end{bmatrix}$$

Figure 3.3: Sobel's two 3x3 gradient kernels.

For each gradient the magnitude and vector angle can be calculated using equa-

tions (3.1) and (3.2). However, pixel-wise orientation is very sensitive to noise in the fingerprint image and therefore is too detailed and somewhat inaccurate. The solution is to calculate block-wise averages of the pixel gradients. This is done in the next section.

$$G = \sqrt{{\delta_x}^2 + {\delta_y}^2} \tag{3.1}$$

$$\theta(i,j) = \frac{\pi}{2} + \arctan(\sqrt{\frac{\delta_x(i,j)}{\delta_y(i,j)}}) \tag{3.2}$$

3.2.2.2 Block-wise Ridge Orientation

Block-wise averages of gradients have multiple purposes when processing fingerprint images. Typically the orientation (or gradients) of each pixel is first smoothed using an averaging filter from a larger area of the image before assigning block-wise orientation averages. The same averaging technique is used in both cases.

Yoon *et al* [YFJ12] use a 16×16 averaging filter to smoothen the pixel-wise orientations prior to computing the block-wise orientations.

The equations for calculating the block-wise orientations for each block are given where pixel (i,j) is the centre of the block being calculated. Equations (3.3) and (3.4) show the two components, V_x and V_y, of the doubled local ridge orientation vector [Rav90]. W is the block size, Yoon, S. *et al* [YFJ12] use 8×8 pixel blocks. Calculating the dominant ridge flow is in equation (3.5) [MMJP09].

$$V_x(i,j) = \sum_{u=i-\frac{W}{2}}^{i+\frac{W}{2}} \sum_{v=j-\frac{W}{2}}^{j+\frac{W}{2}} 2\delta_x(u,v) \cdot \delta_y(u,v) \tag{3.3}$$

$$V_y(i,j) = \sum_{u=i-\frac{W}{2}}^{i+\frac{W}{2}} \sum_{v=j-\frac{W}{2}}^{j+\frac{W}{2}} (\delta_x(u,v)^2 - \delta_y(u,v)^2) \tag{3.4}$$

$$\theta(i,j) = \frac{\pi}{2} + \frac{1}{2} arctan2(V_y(i,j), V_x(i,j)) \tag{3.5}$$

3.2.3 Orientation Field Approximation

The global orientation field, $\theta(x,y)$, is approximated by a polynomial model to obtain $\hat{\theta}(x,y)$. The cosine and sine components of the doubled orientation at

(x, y) can be represented by bivariate polynomials of order n:

$$g_c^n(x,y) \triangleq \cos 2\theta(x,y) = \sum_{i=0}^{n}\sum_{j=0}^{i} a_{i,j}x^j y^{i-j} \tag{3.6}$$

$$g_s^n(x,y) \triangleq \sin 2\theta(x,y) = \sum_{i=0}^{n}\sum_{j=0}^{i} b_{i,j}x^j y^{i-j} \tag{3.7}$$

where $a_{i,j}$ and $b_{i,j}$ are the polynomial coefficients for $g_c^n(x,y)$ and $g_s^n(x,y)$, respectively [YFJ12].

The order of the polynomial model, n, is selected to be 6. Coefficients $a_{i,j}$ and $b_{i,j}$ for the approximated polynomials $\hat{g}_c(x,y)$ and $\hat{g}_s(x,y)$, respectively, can be estimated by the least squares method.

The approximated orientation field, $\hat{\theta}(x,y)$, is constructed by

$$\hat{\theta}(x,y) = \frac{1}{2}\tan^{-1}\left(\frac{\hat{g}_s(x,y)}{\hat{g}_c(x,y)}\right) \tag{3.8}$$

3.2.4 Orientation Error Map

Globally, a good quality fingerprint has smooth orientations except near singular points, the approximated orientation field will therefore generally model the estimated orientation field quite well.

Altered areas in a fingerprint, e.g. around scars and obliterated areas, can result in discontinuous or unnatural changes in the orientation field. The approximated orientation field will not be able to accurately represent these abrupt and irregular changes caused by alterations.

An error map, $\epsilon(x,y)$, is therefore computed as the absolute difference between $\theta(x,y)$ and $\hat{\theta}(x,y)$.

$$\epsilon(x,y) = min(|\theta(x,y) - \hat{\theta}(x,y)|, \pi - |\theta(x,y) - \hat{\theta}(x,y)|)/(\pi/2) \tag{3.9}$$

The error map shows how precise the approximation is to the estimation. Abrupt changes and discontinuities in the ridge flow will result in high values in the error map.

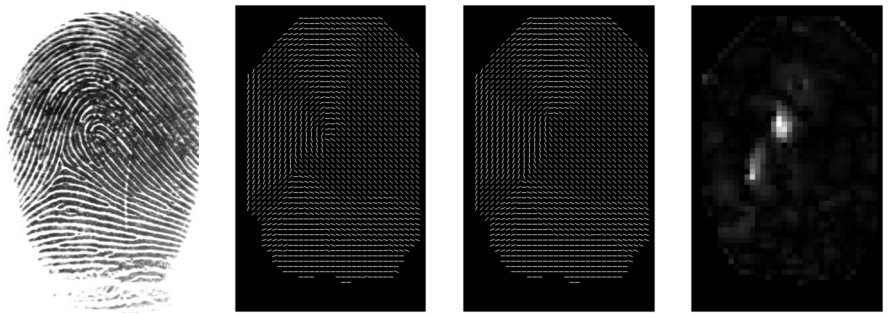

(a) Original (b) Estimation (c) Approximation (d) Error map

Figure 3.4: OFA of an unaltered fingerprint. The error map has high values around singularities. Source of original fingerprint image: [CMM+04].

Unaltered fingerprints of good quality will therefore only have small errors around singular points, whereas altered fingerprints can additionally have errors in scarred or mutilated areas. Figures 3.4 and 3.5 illustrate the resulting orientation fields and error map of an unaltered fingerprint and an altered fingerprint, respectively.

In order to extract features for classification using SVM, a feature vector is constructed from the error map. It is done in the following manner:

1. Two columns of blocks are removed from each side of the error map which results in an error map of size 60×60 blocks.
2. The error map is divided into 3×3 cells. The size of each cell is therefore 20×20 blocks.
3. Histograms in 21 bins in the range [0,1] are computed for each of the nine cells.
4. The nine histograms are concatenated into a 189-dimensional feature vector.

3.3 Minutiae Distribution Analysis

One of the main characteristics that is used by AFIS for comparing fingerprints are *minutiae*. Minutiae are located at ridge endings or ridge bifurcation. In

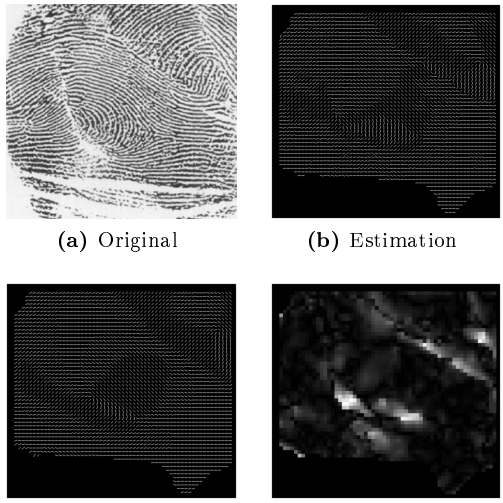

(a) Original **(b)** Estimation

(c) Approximation **(d)** Error map

Figure 3.5: OFA of an altered fingerprint. The approximation is unable to correctly model abrupt changes around distorted areas. The error map therefore has high values around singularities and in some scarred regions. Source of original fingerprint image: [Wer98].

this analysis the minutiae extractor *Mindtct* in NBIS [WGTW12] is used to extract minutia from a fingerprint. Chapter 7 has a more in-depth description of minutiae and also the minutiae extractor.

The analysis is based on the observation that the minutiae distribution of altered fingerprints often differs from that of natural fingerprints [YFJ12]. The analysis constructs a density map of the minutiae points by using the Parzen window method with uniform kernel function.

Let $\mathbf{S_m}$ be the set of minutiae of the fingerprint, i.e.,

$$\mathbf{S_m} = \{\mathbf{x} \quad | \quad \mathbf{x} = (x, y) \text{ is the position of minutia}\}. \tag{3.10}$$

The density map of the minutia is constructed as follows:

1. The initial minutia density map, $M'_d(\mathbf{x})$, is obtained by

$$M'_d(\mathbf{x}) = \sum_{\mathbf{x_0} \in \mathbf{S_m}} K_r(\mathbf{x} - \mathbf{x_0}), \tag{3.11}$$

where $K_r(\mathbf{x} - \mathbf{x_0})$ is a uniform kernel function centered at $\mathbf{x_0}$ with radius, r. Yoon *et al* [YFJ12] set the radius to 40 pixels. However, the current implementation of this algorithm made for this thesis uses $r = 30$, since this gave better results.

2. The initial density map, $M'_d(x, y)$ is smoothed by a Gaussian filter (30×30 pixels) with a standard deviation of 10 pixels.

3. $M_d(x, y)$ is transformed to lie in the interval $[0, 1]$ by

$$M_d(x, y) = \begin{cases} M'_d(x, y)/T, & \text{if } M'_d(x, y) \leq T, \\ 1, & \text{otherwise} \end{cases} \tag{3.12}$$

where T is a predetermined threshold (T is set to 6.9 in this specific implementation).

Figures 3.6 and 3.7 show the density maps of an unaltered and altered fingerprint, respectively. Alterations will cause ridge discontinuities which will result in many spurious minutiae.

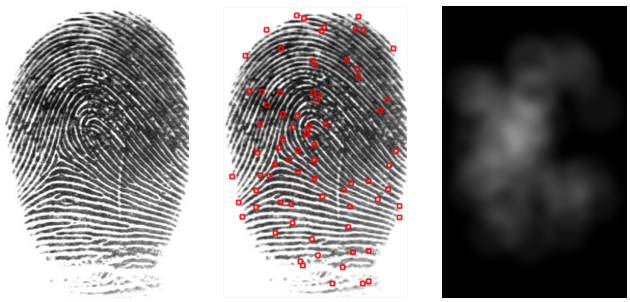

(a) Original **(b)** Minutiae **(c)** Density map

Figure 3.6: Minutia density map of an unaltered fingerprint. Source of original fingerprint image: [CMM+04].

A feature vector is also constructed from the density map in the same fashion as in the OFA. 16 columns of pixels are removed from each side of the density map, resulting in an image of size 480×480 pixels. The density map is divided into 3×3 cells, where each cell is 160×160 pixels.

Histograms of each cell of the density map are computed in 21 bins in the range $[0, 1]$. The nine histograms are concatenated to construct a 189-dimensional feature vector.

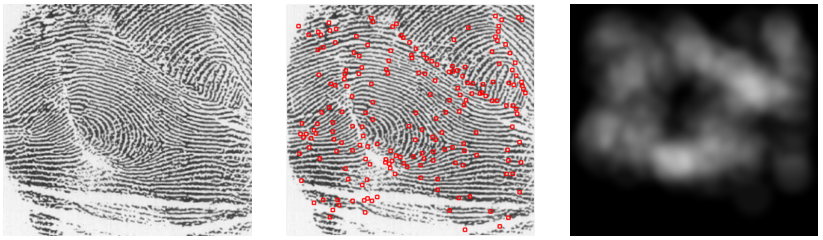

(a) Original **(b)** Minutiae **(c)** Density map

Figure 3.7: Minutia density map of an altered fingerprint. Source of original fingerprint image: [Wer98].

The feature vector from the OFA is concatenated to the feature vector from the MDA. This gives a feature vector of 378 dimensions. The feature vector is fed into a SVM for classification.

3.4 Summary

The state-of-the-art algorithm described in this chapter is based on two different analyses of a fingerprint image: Orientation Field Analysis (OFA) and Minutia Distribution Analysis (MDA).

The OFA identifies discontinuities in the orientation field. This is done by approximating the orientation field using a pair of bivariate polynomials. The differences of the initial estimated orientation field and the approximated field will highlight abrupt changes in the orientation field.

The MDA creates a minutiae density map in order to represent the distribution of minutiae. Discontinuities in friction ridges of altered fingerprints will generally result in a higher density of minutiae in altered regions.

Feature vectors are extracted from the two analyses, concatenated into one vector and fed into a SVM for classification.

Chapter 4

Proposed Method

The goal of this thesis is to explore the possibilities of defining an alternative approach of the given problem. The following part of the thesis will consider a new method based on analyses of characteristics and features in local areas of a fingerprint in order to detect if a fingerprint has been altered or not.

This chapter will give a brief introduction and overview of the proposed method. In-depth descriptions and analysis of the individual parts of the approach will be given in the following chapters.

4.1 Algorithm Overview

The existing alteration detection algorithm which was described in the previous chapter takes a global approach. It uses polynomials to approximate the orientation field in order to analyse the flow of the ridges and constructs a density map to analyse the minutiae distribution. This thesis will propose a new method which is based on local analysis of pixel-wise orientations and also local analysis of minutiae.

A rough overview of the upcoming algorithm is given in Figure 4.1. The algo-

rithm starts by preprocessing the fingerprint image before branching into two analyses of distinct fingerprint attributes. Features will be extracted from each analysis, fused into one feature vector and thereafter fed into an SVM for classification.

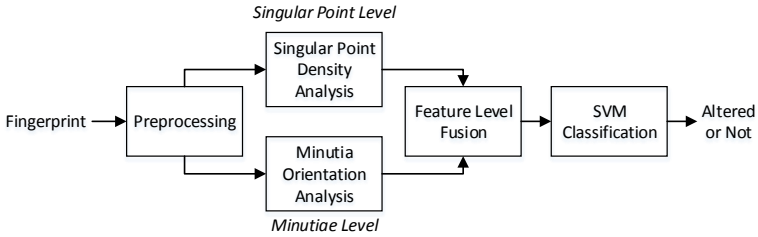

Figure 4.1: Flowchart of the proposed algorithm.

The following sections will give an introduction to the main steps of the method. Extensive descriptions of the preprocessing pipeline and the two analyses will be conducted in the forthcoming chapters.

4.2 Preprocessing

Preprocessing prepares the raw input fingerprint image for the impending analyses. This step locates the fingerprint image, separates foreground from the background, ensures that output images are invariant with respect to translation and rotation, and enhances the input image in order to clarify ridges and reduce undesirable noise.

It is important that the preprocessing pipeline is tailored specifically for the subsequent analyses. The preprocessing pipeline will be explained in chapter 5.

4.3 Singular Point Density Analysis

The singular point density analysis inspects changes in the pixel-wise orientation field. It is based on the local entropy and uncertainty of orientations around scarred and mutilated areas and uses common techniques to extract core features of a fingerprint.

Local areas of high curvature will be found using the Poincaré index. This is

a common method for extracting singular points in which some altered regions share similar characteristics.

Quality measurements of friction ridges are merged into the analysis in order to diminish the effect of uncertainties in poor quality or heavily obliterated areas. Gabor filters will be used to evaluate the quality of ridges.

The analysis will produce a density map in which features will be extracted to feed into the SVM. The extraction of features is described in section 4.5, below.

Chapter 6 will give a detailed description of the analysis. It will consider the steps taken for constructing the final feature density map.

4.4 Minutia Orientation Analysis

Fingerprint alteration significantly affects the distribution of minutiae by severe skin distortion introduced during the process of alteration [YZJ12]. Abrupt ridge endings produced by scars and unusual ridge patterns formed by mutilation will result in additional spurious minutiae.

The state-of-the-art method already demonstrates that altered fingerprints can be detected by analysing the distribution of the minutia. The additional spurious minutia that is caused by alterations will be located along edges of the critical areas. The proposed method will make additional local analysis of each detected minutia in order to identify discontinuities and changes in the orientation.

The nature of the analysis will require slight modifications of the minutiae extractor. Chapter 7 gives a detailed description of these modifications together with a thorough examination of the analysis.

As with the singular point density analysis, the chapter will conclude with the construction of a density map. Extracting the features from the map in order to construct a feature vector for the SVM is given below in section 4.5.

4.5 Feature Extraction

There are multitudes of different ways of analysing data and extracting features to be used by an SVM. The feature extraction is based on the exact same

properties and methods as the previous state-of-the-art approach. Some of the reasons are the following:

- Both of the proposed analysis algorithms are reliant on the distribution of special features across the fingerprint in a similar fashion to the predefined method.
- It is built on a proven technique.
- Will provide additional interoperability in the testing of the algorithms. Each analysis is interchangeable since they provide a common data format such that feature extraction and interpretation of the results share a common ground.

The final density maps from each analysis are images in the size of 512×480 pixels with intensity values that are normalised to lie in the range of $[0, 1]$. The feature extraction will construct a 189-dimensional vector from each analysis. This is done as follows:

1. Columns of 16 pixel are removed from each side of the density map. This gives a density map of size 480×480 pixels.
2. In order to separate and extract features from different sections of the image it is divided into 3×3 cells. The size of each cell is thus 160×160 pixels.
3. Histograms in 21 bins in the range [0,1] are computed for each of the nine cells.
4. The nine histograms are concatenated into a 189-dimensional feature vector.

The two feature vectors are fusioned by concatenation which results in a 378-dimensional feature vector. The feature vector is fed into a SVM for classification.

4.6 Summary

A method will be proposed which is based on localised analyses of two different attributes of the fingerprint image. It is constructed in a similar fashion as the

existing alteration detection algorithm. This will make the different analyses interchangeable such that testing and benchmarking can easily be performed.

The proposed solution uses a SVM for classification. Feature vectors are constructed from the two analysis and fed into the SVM.

The following chapters will give a detailed description of the different parts of the proposed alteration detection method.

Chapter 5

Preprocessing Pipeline

Preprocessing serves an essential part when analysing and extracting features from a fingerprint image. Preprocessing deals with the subject of enhancing the quality of an image and preparing it for being processed, in this case, by alteration detection algorithms.

A raw fingerprint image is input into the preprocessing pipeline. The pipeline is used to identify foreground and background of the image, to reduce noise and increase the contrast between ridges and valleys, and to transform the image into a common and "invariant" format. The output should thus be a fingerprint image with properties and enhancements specifically designed for the following analysis process.

Figure 5.1 shows the five steps of the preprocessing pipeline. The pipeline consists of the following:

1. Cropping. Locating and isolating the fingerprint image.
2. Segmentation. Separating the foreground from the background.
3. Rotation. Align fingerprint image along the longitudinal direction.
4. Resize. The size of the image is changed to fit a specified size.

5. Enhancement. Improve the clarity of friction ridges and minimize noise.

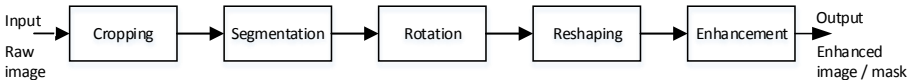

Figure 5.1: Main steps of preprocessing pipeline.

This chapter will describe the steps of the preprocessing pipeline in order to prepare fingerprint images for fingerprint alteration detection analysis. Also, an alternative enhancement method will briefly be discussed in the final part of the chapter.

5.1 Cropping

The NIST Biometric Image Software (NBIS) [WGTW12] includes a fingerprint segmentation algorithm, *Nfseg*, for cropping a rectangular region of an input fingerprint. The core strengths of *Nfseg* are to segment the four-finger plain impression found on the bottom of a fingerprint card into individual fingerprint images. However, it can also be used on single fingerprint images.

Nfseg is used to locate the fingerprint and remove excessive white space from the input fingerprint. Since it does not do a good job of aligning the fingerprint along the longitudinal direction, further rotation techniques will be used further on in the pipeline.

5.2 Segmentation

An important image preprocessing operation is that of separating the fingerprint image ridge area – the Region Of Interest (ROI) – from the image background. This is known as fingerprint segmentation.

The input fingerprint image, I, is intensity normalised to have zero mean along with unit standard deviation. This is done by the following pixel-wise function:

$$\forall x \in \{1..R\}, y \in \{1..C\} : I_n(x,y) = \frac{I(x,y) - avg(I)}{std(I)} \tag{5.1}$$

where $avg(I)$ is the average pixel intensity of the input image and $std(I)$ is the standard deviation. $I(x, y)$ is the pixel intensity at pixel (x, y) of the input image.

From I_n it is possible to generate a binary image, I_{mask}, known as the *mask* of the fingerprint where ones belong to the image ROI and zeros belong to the background.

The normalised image is divided into blocks of size 8×8. If the standard deviation of a block is above a threshold, T, then the block is regarded as being part of the actual fingerprint, i.e. the foreground. This is a block-wise process; the function for creating the mask is the following:

$$Ib_{mask}(x, y) = \begin{cases} 0 & \text{if } std(Ib(x, y)) \leq T, \\ 1 & \text{otherwise} \end{cases} \tag{5.2}$$

where Ib contains the blocks of size 8×8 pixels. The threshold, T, is set to 0.1.

Morphological operations are run on the block-wise mask image, Ib_{mask}, for filling holes and removing isolated blocks yielding Ib'_{mask}. This is done by first running a series of open operations (erosion followed by a dilation) for filling holes. Thereafter a series of close operations (dilation followed by an erosion) are run to remove isolated blocks.

Two different structures are used for the morphological operations: a square rotated 45° with a diagonal length of 5 blocks and a square with a length of 3 blocks. The series of open operations are conducted by alternating between the two shapes, starting with the rotated square. The close operations are executed in the same fashion, however starting with the *unrotated* square. The shapes have been set empirically.

An additional erosion operation using the same disk-shape element is used to ensure that border blocks that may hold part background and part foreground are eliminated.

The final pixel-wise fingerprint mask, I_{mask}, is the up-scaled version of the final block-wise mask, Ib'_{mask}. An example of the segmentation can be seen in Figure 5.9.

This is quite an aggressive segmentation which is well suited for detecting if a fingerprint has been altered or not. The strengths are that it removes unclear borders which might be identified as altered while keeping low quality areas that reside within the ROI.

(a) Original (I) **(b)** Ib_{mask} **(c)** Final mask (I_{mask})

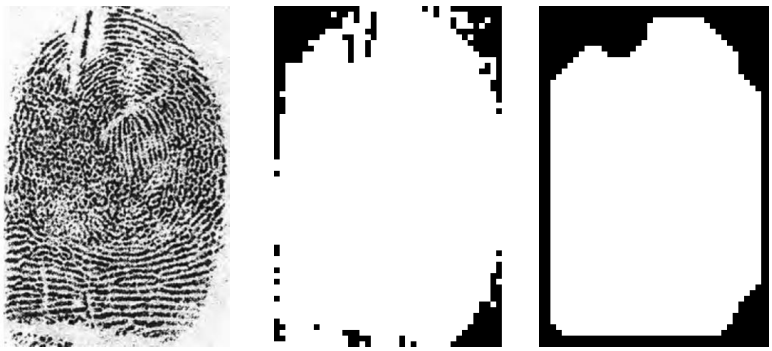

(d) Original (I) **(e)** Ib_{mask} **(f)** Final mask (I_{mask})

Figure 5.2: Segmentation of two fingerprint images. Source: (a) [CMM+04], (d) [Sam01].

Likewise, this segmentation is not ideal for fingerprint recognition purposes since too many foreground blocks would be removed possibly erasing important minutiae. Low quality areas within the fingerprint can also add unwanted minutia or features that can compromise the comparison algorithm whereas they will play an important part in determining if the image has been altered or not.

5.3 Rotation

The goal is to rotate the fingerprint image so that it is aligned along the longitudinal direction of the finger.

Some landmark of the fingerprint image is normally used as a reference point for rotation purposes. Different approaches have been proposed for rotating a fingerprint image, such as computing the image orientation using singular points as reference points (e.g [LJK05]), using the fingerprint Center Point Location (CPL) as a reference point (e.g. [MIK+10], [MLBM11]) or using minutiae as reference points [JA07].

Using minutia or singular points as reference points requires significant analysis of the fingerprint image and can be quite complex. The approach taken in this thesis is based on [MIK+10] since it is a simple and efficient approach which does not require complex computations. The approach is built on the assumption that most fingerprints have an ellipsoidal shape.

As mentioned earlier, the method uses the fingerprint CPL as a reference point for rotation. Since the core point is a consistent point at the central point of the fingerprint the core can be used as the CPL [JPH99]. However, since this requires analysis of the actual fingerprint image, Merkle *et al* [MIK+10] uses the centroid of the ROI instead.

The proposed rotation method therefore uses the *mask* of the fingerprint which was constructed in the previous step. The mask, as described in 5.2, is a binary image denoting fingerprint foreground as ones and background as zeros. To increase computation speed the mask of the fingerprint image is scaled down, in this current implementation by a factor of eight. The image is shifted so that the centroid of the ROI is at point $(0, 0)$.

Consider the image being placed in a Cartesian coordinate system, see Figure 5.3. Two areas, a_1 and a_2 are defined where a_1 is composed of quadrant 2 (upper left) and 4 (bottom right) while a_2 is composed of the remaining diagonal quadrants.

The idea is to rotate the foreground image around the center so that the amount of foreground pixels is balanced between a_1 and a_2.

This is an iterative process. Let $s(a_i)$ denote the sum of pixels in area a_i. If $s(a_1) > s(a_2)$ then the image is rotated clockwise by 1°, otherwise the image is rotated counter-clockwise by 1°. The iteration stops once the direction of rotation changes, e.g. the balance of the sum is shifted to the opposite quadrants.

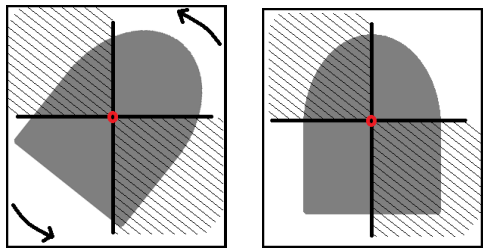

(a) Original **(b)** After rotation

Figure 5.3: The fingerprint mask is placed in a coordinate system and rotated. The sums of the fingerprint foreground of the quadrants with the patterned background are compared to the sums of the quadrants with a clear background.

The aggregated rotations are applied to the original fingerprint image.

This rotation is adequate considering that input fingerprint images normally are aligned within $\pm 45°$ of the longitudinal direction of the finger. However, if the fingerprint is $\pm 90°$ from the intended direction, the final rotation will result in the fingerprint image being rotated upside down.

A great weakness of the current rotation method is that it is not always able to handle fingerprint images where the outline is not somewhat ellipsoidal or even. This can happen if a large area is of a poor quality and is conceived to be background. The current solution is to have a maximum rotational angle of $\pm 45°$; rotations past these thresholds are set to $0°$.

5.4 Resizing

The fourth step is the very simple process of resizing the image. It is important that features that will be extracted from the fingerprint images in the subsequent analyses are invariant with respect to size, translation and rotation. This step is the final and critical process in ensuring that this criteria is fulfilled.

Before resizing, the image must be cropped again since rotation might have added additional background to the sides of the image. There are many ways that the image can be re-cropped, e.g. by using the *Nfseg* algorithm or removing columns and rows that contain only zeros. The current implementation uses a simple approach cropping the fingerprint image based on the rotated orientation

mask.

The image is resized to the closest fit for 512×480 pixels and thereafter segmented afresh.

5.5 Enhancement

The final step of the preprocessing pipeline is enhancement of the fingerprint image. The goal of fingerprint enhancement techniques are traditionally to improve the clarity of friction ridges and remove unwanted noise in order to assist the following analyses or feature extraction algorithms.

Numerous fingerprint enhancement techniques have been proposed, section 5.6 will briefly compare some methods to support the final choice of enhancement algorithms. This section will briefly describe the chosen algorithms.

Two processes were conducted on the image to slightly enhance it: histogram equalisation in the spatial domain and a simple enhancement in the frequency domain. These methods will be described in the following sections.

5.5.1 Histogram Equalisation

Histogram equalisation is a common method for enhancing the contrast of a image. The method defines a mapping of grey levels p into grey levels q which attempts to uniformly distribute the grey levels q [Jai89]. A cumulative histogram of the enhanced image would show a relatively linear curve and the ideal mean would be right in the centre of the density value. Histogram equalisation is described in equation (5.3) where k is the grey scale level of the original image, n_j is the number of times pixel value j appears in the image, n is the total number of pixels and L is the number of grey levels (for example 256).

$$\forall i \in \{1..R\}, j \in \{1..C\} : G(i,j) = H(I(i,j)) = H(k) = \sum_{j=0}^{k} \frac{n_j}{n}(L-1) \quad (5.3)$$

The contrast of grey levels are stretched near the histogram maxima using histogram equalisation. This improves the detectability of many image features [KP02].

A limitation with a global histogram equalisation on a fingerprint is that it sometimes can enhance noise since the colour distribution of a fingerprint image is not necessarily uniform. For example if white is the dominant colour in an image, then the very light grey colours would be "moved" relatively far towards the darker grey. Applying this technique only on the ROI or maybe even using a block-wise approach of this method would probably yield better results.

This limitation of the histogram equalisation is not a large problem in this particular enhancement scheme, since the fingerprint itself has been localised and cropped prior to the histogram equalisation. This limits the amount of background pixels in the image which otherwise could contribute to the excessive change in brightness.

5.5.2 Enhancement in the Frequency Domain

The smooth and continuous orientation of the friction ridges in a fingerprint together with consistent friction ridge characteristics, such as ridge and valley widths, give fingerprint images a special characteristic in the frequency domain.

Ridges can be locally approximated by single sine waves. The orientation of the ridges gives frequencies in all directions. A good quality fingerprint image will therefore produce a clear ring pattern around the center in the frequency domain (see Figure 5.4). The clearness of the ring is based on the consistency of the the ridge characteristics.

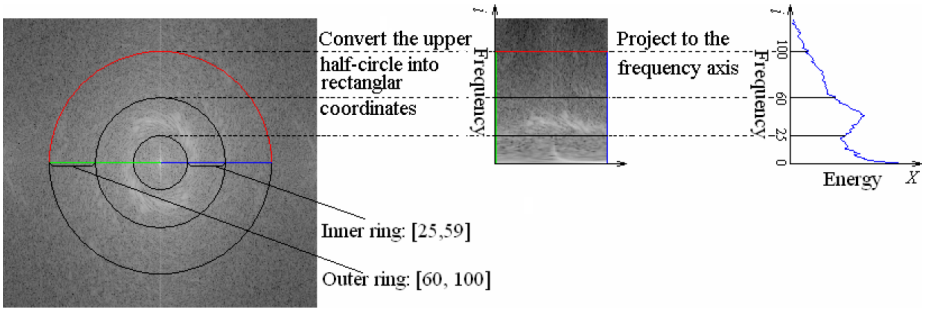

Figure 5.4: Fingerprint images produce a ring pattern in the frequency domain. Note the spectral energy in the *inner ring*. Source: [JKE07].

The NFIQ 2.0, which is currently under development, uses a radial power spectrum to determine a quality score of the fingerprint [NIS12]. The quality score is based on the peak of maximum energy in the *inner ring*. This can also be seen in Figure 5.4.

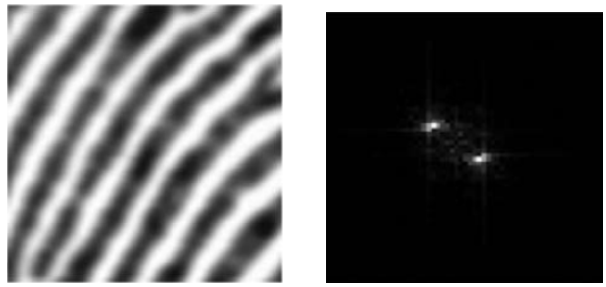

(a) Ridges in local area **(b)** Frequency domain of (a)

Figure 5.5: Orientation and frequency of ridges in local area. Source: [CCG05]

One method of improving the clarity of the ridge patterns could be to apply a filter which enhances the frequencies in the inner ring while minimising or even eliminating frequencies outside of the inner ring.

Altered fingerprints will have unnatural ridge properties on a global scale and – depending on the type of alteration – be of a less quality. It is desired to also enhance discrepancies since the impending analyses will be on these inconsistencies.

Watson *et al* [WCG94] presented a simple enhancement method based on enhancing dominant frequencies in the frequency domain. This method concentrates on local properties and is performed using overlaying blocks. This approach will be used to enhance fingerprint images in this thesis. The local parallel ridges and valleys in a fingerprint have a well-defined local frequency and orientation [JPHP00], see Figure 5.5. The enhancement method takes advantage of this property.

This method is quite efficient in enhancing the image for the specific purpose of analysing altered fingerprints. The reason being that it manages to fill up small holes in ridges and also otherwise enhance the appearance of the friction ridges in otherwise good quality areas. At the same time scattered frequencies in low quality areas, such as in scarred and mutilated areas, tend to further enhance the friction ridge uncertainties in those areas.

The fingerprint image is divided into blocks of size 8×8 pixel. An additional overlapping border of 8×8 pixels is added around each block such that the actual size of each block is 24×24 pixels. The Fast Fourier Transform (FFT) of each block is multiplied by an exponentiation of its magnitude; the exponent factor k is set to 0.45. The enhanced block $B'(x, y)$ based on the original block

(a) Original (I) **(b)** Enhanced (I_{enh}) **(c)** Mask (I_{mask}) **(d)** Final image

Figure 5.6: Enhancement of an unaltered fingerprint. Source: (a) [CMM+04].

$B(x, y)$ is done accordingly:

$$B'(x, y) = FFT^{-1}(FFT(B(x, y)) \cdot |FFT(B(x, y))|^k) \tag{5.4}$$

Notice that in Equation 5.4 blocks $B(x, y)$ and $B'(x, y)$ are 24×24 pixels, i.e. they are extended by the borders. The enhanced image, I_{enh}, is combined by the centre 8×8 pixels in each block of B'. Examples of the resulting enhancements on altered and unaltered fingerprint images can be seen in Figures 5.6 and 5.7, respectively. The reason for using overlapped blocks is to minimise the border effect of the block-wise FFT.

The idea of the method is that dominant frequencies of each block correspond to the ridges, amplifying these dominant frequencies increases the ratio of ridge information to non-ridge noise [WCG94].

Willis and Myers [WM01] suggested using a larger value for k, e.g. 1.4, together with larger blocks. This increases the power of the reconstruction. For analysing altered fingerprints it was found more effective using a smaller k together with smaller blocks, since this slightly improves the ridge quality but does not artificially reconstruct larger areas of the fingerprint.

5.6 Alternative Enhancement Methods

Many different methods and techniques have been proposed to enhance fingerprints, some examples are the following:

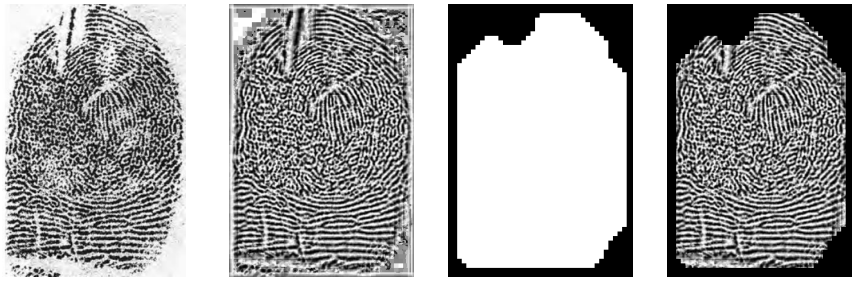

(a) Original (I) **(b)** Enhanced (I_{enh}) **(c)** Mask (I_{mask}) **(d)** Final image

Figure 5.7: Enhancement of a altered fingerprint. Source: (a) [Sam01].

- Hong *et al* [LHJ98b] proposed a method using Gabor filters based on estimates of local friction ridge characteristics, such as orientation and frequency. Yang *et al* [YLJF03] proposed a modified method based on this approach which was slightly more accurate in preserving the fingerprint image topography.

- Enhancements in the frequency domain have been proposed. Chikkerur *et al* [CCG05] suggested a method based on Short Time Fourier Transform (STFT). Similarly Sherlock *et al* [SMM94] also proposed a method using a set of directional filters in the Fourier domain.

- Many methods have also been proposed using wavelet transforms, such as [HLW03], [YMY07], [HHKA05] and [ZWT02]. A common method, based on the same ideas as some of the above enhancements, is to use a set of directional filters.

It is important that the choice of enhancement algorithm complements the alteration detection algorithms. Even though the alteration detection algorithms have not been explored yet, some preferences of the attributes of enhancement algorithms can already be determined. Compared to traditional minutia extraction methods used for fingerprint matching purposes; the selected algorithm should retain some local inconsistencies.

Many of the above mentioned techniques are able to reconstruct and rejoin ridges that have been broken or unclear. This is basically done using local analysis of the fingerprint characteristics. Analysing if a fingerprint has been altered or not requires analysing discrepancies and irregularities, the extent of reconstruction is therefore also an issue.

An implementation based on the Gabor filter approach which was proposed by Hong *et al* [LHJ98b] was compared with the proposed enhancement method in the frequency domain. An in-depth description of the algorithm will be left out of this report. However, the main idea will briefly be described.

Figure 5.8 shows the main concepts of the algorithm. The image is divided into blocks of size 16×16. An *oriented window* of size 32×16 is calculated for each of these blocks and rotated to match the estimated orientation of the given block. The frequency of the ridges and valleys in the oriented window is analysed giving a so-called *x-signature*. The x-signature forms a discrete sinusoidal-shape wave with the same frequency as the ridges and valleys in the oriented window. A Gabor filter based on the x-signature and orientation is applied to the processed block.

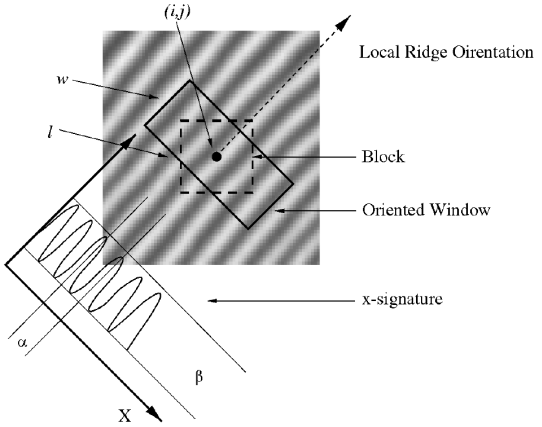

Figure 5.8: A block is enhanced using a Gabor filter based on the *x-signature* and orientation of the local ridge characteristics. Source: [LHJ98b].

According to Hong *et al* [LHJ98b] the algorithm is designed to only run on recoverable parts of the fingerprint, e.g. areas that are deemed to be part of the foreground. Unrecoverable areas that contain severe noise or distortion so that it does not provide enough information about the true friction ridge structures would be segmented out. This conflicts somewhat with the desired enhancement, which is also to slightly enhance altered areas of the fingerprint. These areas might be unrecoverable.

As seen in Figure 5.9 the Gabor filter method is efficient in rejoining ridges that have been broken by creases or smudges. However, running the algorithm on unrecoverable areas, such as highly obliterated areas (Figure 5.9f), results in the reconstruction of friction ridges in random orientations.

The proposed enhancement method is not as efficient in joining broken friction ridges as the Gabor filter method. However, it manages to enhance the appearance of both recoverable and unrecoverable areas.

(a) Original (I) **(b)** Proposed method **(c)** Gabor method

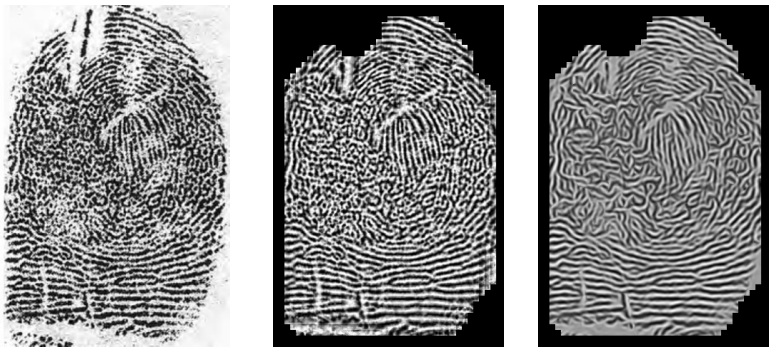

(d) Original (I) **(e)** Proposed method **(f)** Gabor method

Figure 5.9: Gabor filter enhancement [LHJ98b] tries to reconstruct missing ridges, while the proposed enhancement method only joins ridges in relatively clear areas. Source: (a) [CMM+04], (f) [Sam01].

5.7 Summary

The preprocessing pipeline plays an important part in processing and analysing fingerprint images. The main purpose of the preprocessing pipeline is to prepare a raw fingerprint image for the actual processing, e.g. analyses, feature extraction or alteration detection. The central processing algorithm is highly dependent on the quality of the input and will give different results depending on the condition of the input fingerprint image.

The succeeding alteration detection algorithms rely on the preprocessing pipeline to deliver fingerprint images with clear friction ridge patterns in recoverable or well-defined areas while maintaining enhanced characteristics in unrecoverable areas. Also, images fed to the alteration detection algorithms should be invariant with respect to translation and rotation.

The main functions of the preprocessing pipeline can be summarised as:

- Cropping and reshaping to ensure that the fingerprint image is invariant with respect to translation and rotation.
- Segmentation to separate the foreground, ROI, from the background.
- Enhancement to clarify the appearance of friction ridges.

Chapter 6

Singular Point Density Analysis

Scars and other deformation of the fingerprint caused by alteration causes unnatural changes in the orientation field both globally, as analysed by the alteration detection algorithm proposed by Yoon *et al* [YFJ12], and also locally. Scars will have unnatural joint friction ridges while other obfuscation causes various random noisy patterns in the friction ridges.

The proposed method, Singular Point Density Analysis (SPD), for analysing if a fingerprint is altered or not is based on local analysis of the orientation field using the Poincaré index to detect noisy friction ridge areas. An altered fingerprint will have a higher density of such areas than an unaltered.

6.1 Pre-Analysis

Singular points, called core and delta, act as control points around which the ridge lines are "wrapped" [MMJP09]. The core is defined as the *topmost point on the innermost recurving ridgeline of a fingerprint* [ISO11] while a delta is a *point on a ridge at or nearest to the point of divergence of two typelines and*

located at or directly in front of the point of divergence [ISO11]. Figure 6.1 illustrates the locations and typical characteristics of core and delta points.

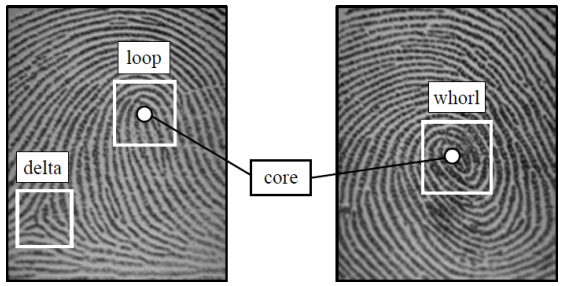

Figure 6.1: Delta and core points in fingerprint images. Source: [MMJP09].

The suggested approach is partly inspired from research done by Petrovici [PL10b]. The research calculates amplitudes of singular points based on the reliability of their orientation. Experimental results on synthetically altered images indicate that altered fingerprints will have many singular points with lower amplitudes while unaltered fingerprints have a few singular points with higher amplitudes.

Before describing the actual method, a brief analysis of the characteristics of the orientation field will be conducted on altered and unaltered images.

6.1.1 Orientation Certainty Level

The Orientation Certainty Level (OCL) is a common analysis used as a quality measure to determine the certainty of local orientations. It measures the energy concentration along the direction of ridges [XYYP08].

In section 3.2.2.1 the two intensity gradients, δ_x and δ_y, were found for each pixel using a Sobel operator. This was used to calculate the pixel-wise orientation. The orientation certainty can be calculated as the ratio of the two eigenvalues of the covariance matrix of the gradient vector.

The covariance matrix C of the gradient vector for an N points image block is

given by:

$$C = \frac{1}{N}\sum_{i=1}^{N}\left\{\begin{bmatrix} dx_i \\ dy_i \end{bmatrix}\begin{bmatrix} dx_i & dy_i \end{bmatrix}\right\} = \begin{bmatrix} \frac{1}{N}\sum_{i=1}^{N} dx_i^2 & \frac{1}{N}\sum_{i=1}^{N} dx_i dy_i \\ \frac{1}{N}\sum_{i=1}^{N} dy_i dx_i & \frac{1}{N}\sum_{i=1}^{N} dy_i^2 \end{bmatrix} = \begin{vmatrix} a & c \\ c & b \end{vmatrix} \tag{6.1}$$

where $dx = \delta_x$ and $dy = \delta_y$ are the gradient densities at each pixel.

The eigenvalues, λ_{max} and λ_{min}, can be calculated as[LJY02]:

$$\lambda_{max} = \frac{(a+b) + \sqrt{(a-b)^2 + 4c^2}}{2} \tag{6.2}$$

$$\lambda_{min} = \frac{(a+b) - \sqrt{(a-b)^2 + 4c^2}}{2} \tag{6.3}$$

The OCL is defined in the range $[0, 1]$ where a high value means good quality. The formula for calculating the OCL is therefore:

$$Ocl = 1 - \frac{\lambda_{min}}{\lambda_{max}} \tag{6.4}$$

(a) Original **(b)** Certainty **(c)** Original **(d)** Certainty

Figure 6.2: Two unaltered images and their corresponding orientation certainty. Since the images are of relatively good quality, low certainty is in areas of high curvature. Source: (a), (c) [CMM+04].

Figures 6.2 and 6.3 show images of the pixel-wise OCL of unaltered and altered fingerprints, respectively. This has been calculated using blocks of size 15×15 build around each pixel. The unaltered images are of relatively good quality such that the orientation certainty is mainly high throughout the fingerprint. Only around singular regions is the certainty low. Some medium certainties are

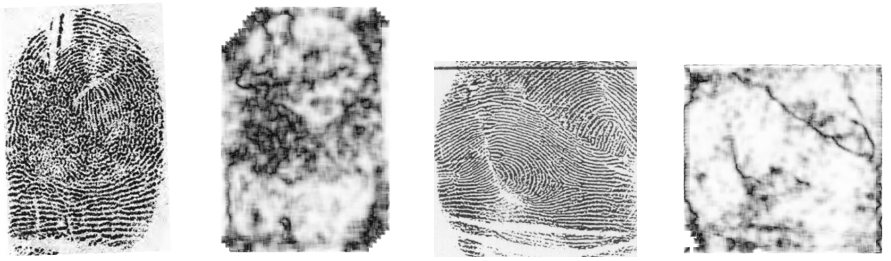

(a) Original **(b)** Certainty **(c)** Original **(d)** Certainty

Figure 6.3: Two altered images and their corresponding orientation certainty. Areas with low friction ridge quality caused by scars and obliteration cause low orientation certainty. Source: (a) [Sam01], (c) [Wer98].

also vaguely seen in Figure 6.3d caused by small discontinuities in the friction ridges.

It comes to no surprise that areas of low quality and scarred areas have a low orientation certainty which can clearly be seen in Figure 6.3. In Figure 6.3d most of the scar from the z-cut alteration is clearly visible.

6.1.2 Orientation Entropy

Entropy is a description to the uncertainty of a random variable; it can therefore be used as a measure of the disorder of variables in a given system.

Considering the pixel-wise orientation, $\theta(x, y)$, as a random variable. Using a sample rate, n, determining the amount of possible orientation values, a quantification scale $\frac{\pi}{n}$ is used to discretise the orientation field. The discrete orientation field, θ_n, with sample rate n can be computed as:

$$\forall x \in \{1..R\}, y \in \{1..C\} : \theta_n(x, y) = \frac{\pi}{n}(\frac{\theta(x, y)}{\frac{\pi}{n}} \mod n) \tag{6.5}$$

where R and C define the row count and column count of the orientation image, respectively.

The orienation entropy is *a measure of how much "choice" is involved in the selection of the event or of how uncertain we are of the outcome* [Sha01]. The entropy for each orientation is calculated according to the amount of different

possibilities in the surrounding area. Blocks of size 5×5 are used in the current implementation, i.e. for each pixel, the surrounding pixels are taken into consideration.

The discrete entropy image, E_n, can be constructed as:

$$\forall x \in \{3..R-2\}, y \in \{3..C-2\} : E_n(x,y) = -\sum_{i=1}^{n} p_{x,y}(\frac{\pi}{i}) \log_{10} p_{x,y}(\frac{\pi}{i}) \quad (6.6)$$

where $p_{x,y}(\frac{\pi}{i})$ is the probability of the discrete orientation $\frac{\pi}{i}$ in the block belonging to (x,y). Since blocks of size 5×5 are used, pixels that don't have a complete border of 2×2 surrounding pixels are not considered.

Figures 6.4 and 6.5 show multiple scaled orientation entropy images of unaltered and altered fingerprint images, respectively.

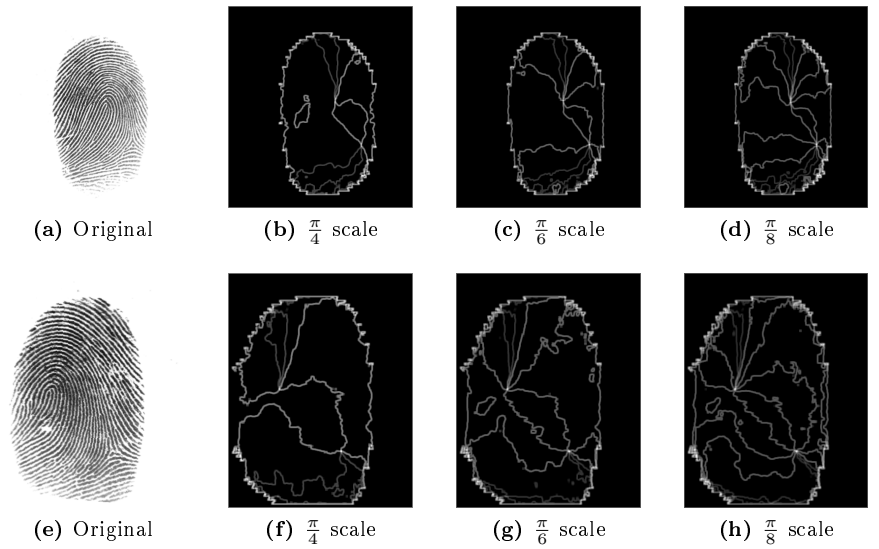

(a) Original **(b)** $\frac{\pi}{4}$ scale **(c)** $\frac{\pi}{6}$ scale **(d)** $\frac{\pi}{8}$ scale

(e) Original **(f)** $\frac{\pi}{4}$ scale **(g)** $\frac{\pi}{6}$ scale **(h)** $\frac{\pi}{8}$ scale

Figure 6.4: Multiple scaled orientation entropy images of unaltered fingerprints. Images have sample rate $n = 4$, 6 and 8. Constant high entropy values are in singular regions where they act as center points. The entropy varies in other positions of the fingerprint according to the scale. Source: (a), (e) [CMM+04].

The characteristics of the entropy images are very distinct in the demonstrated images according to the nature of the fingerprint. The center points in the orientation entropy images which have a constant high entropy value are points

with uncertain orientations. The difference between the entropy values in the illustrated unaltered and altered images can be summarised as:

- Unaltered fingerprint images have a constant high entropy value in the center of singular regions.
- Altered fingerprint images have many spurious positions with a constant high entropy value. Scarred regions and mutilated areas add uncertainties in the pixel-wise orientations which lead to the high entropy values.

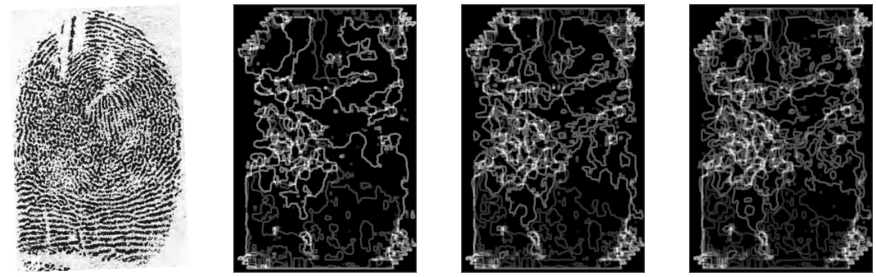

(a) Original **(b)** $\frac{\pi}{4}$ scale **(c)** $\frac{\pi}{6}$ scale **(d)** $\frac{\pi}{8}$ scale

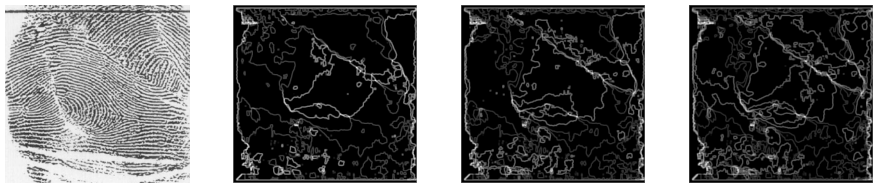

(e) Original **(f)** $\frac{\pi}{4}$ scale **(g)** $\frac{\pi}{6}$ scale **(h)** $\frac{\pi}{8}$ scale

Figure 6.5: Multiple scaled orientation entropy images of altered fingerprints. Images have sample rate 4,6 and 8. Obliterated areas and scars generate high entropy readings. Even with multiple scaled entropy images, there are many central points with a constant high entropy value. Source: (a) [Sam01] , (e) [Wer98].

From Figure 6.4 it becomes clear that it is possible to use the entropy to locate singular points. Chen *et al* [CPL+11] have also shown that combining a series of entropy images of multiple scale by multiplication can be used to locate singular points. Similarly, Tiribuzi *et al* [TPVR12] proposed an approach for detecting altered fingerprints using the minutia density map and multiple-scaled orientation entropy images together with a *Multiple Kernel Learning* framework.

It can be concluded that altered images have a number of positions with a high orientation uncertainty. Based on both the uncertainty and entropy analysis it

seems that altered images have a higher amount of positions in a fingerprint with characteristics similar to singular points.

6.2 Poincaré Index

Methods for detecting singular points are commonly based on the Poincaré index which in this context analyses the change of direction around a given point. Using the Poincaré index for singular point detection was proposed by Kawagoe and Tojo [KT84].

The Poincaré index has shown to have high accuracy, but low robustness [REB10]. Methods to determine singular points relying on local features like Poincaré index or other similar properties of the orientation field work well in good quality fingerprint images. However, they fail to correctly localise reference points in poor quality fingerprints with cracks and scars, dry skin or poor ridge and valley contrast [JPHP00]. Many false core and delta points can be produced when the orientation field is noisy, e.g. in low quality fingerprint areas. The proposed method takes advantage of this limitation.

For correctly detecting singular points different heuristics are used to filter out false locations, e.g. iterative smoothing of the orientation field [BPL08], using a modified gradient based Poincaré method [BG01] and in combination with additional filters [BG02], [ZCG09]. No filtering process will be used in the current analysis which will therefore detect singular point candidates.

In the current context, the Poincaré index for a given point can be defined as the cumulative change in the orientation field travelling clockwise around the neighbouring points, see Figure 6.6.

The pixel-wise orientation field, $\theta(x, y)$ is estimated using the previous defined gradient-based method where $\theta(x, y)$ denotes the orientation of pixel (x, y). The orientation field is smoothed using a 15×15 averaging filter.

For each pixel in the fingerprint ROI the surrounding neighbouring orientations are gathered in order by travelling clockwise around the pixel, starting at any of the eight surrounding pixels. The Poincaré index, $P(x, y)$, calculated for pixel (x, y) with the eight surrounding orientation elements $d_k(k = 0..7)$ is calculated as follows:

$$P(x, y) = \sum_{k=0..7} a(d_k, d_{(k+1) \bmod 8}), \tag{6.7}$$

where $a(d_i, d_j)$ is the angle between d_i and d_j selecting the direction of the

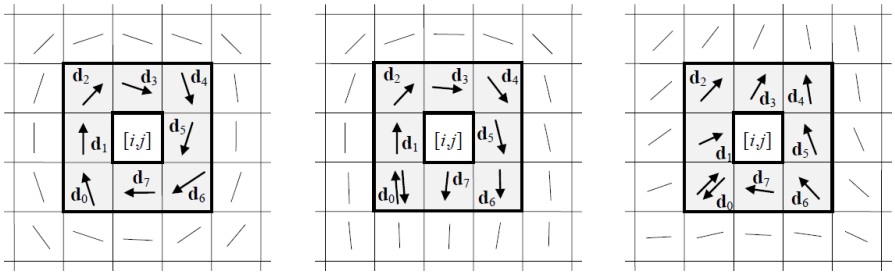

(a) Whorl (360°) **(b)** Loop (180°) **(c)** Delta (-180°)

Figure 6.6: Poincaré index of a given point is the cumulative change in orientation of the neighbouring points, travelling clockwise. Source: [MMJP09].

orientations so that $|d_j - d_i| \leq \pi/2$. The possible values of $P(x, y)$ are 0, $\pm\pi$ and $\pm 2\pi$:

$$P(x,y) = \begin{cases} 2\pi, & \text{if } (x,y) \text{ belongs to a whorl} \\ \pi, & \text{if } (x,y) \text{ belongs to a loop} \\ -\pi, & \text{if } (x,y) \text{ belongs to a delta} \\ -2\pi, & \text{if } (x,y) \text{ is in the center of a rare } \textit{diamond} \text{ shape} \\ 0, & \text{otherwise} \end{cases} \tag{6.8}$$

Notice that a Poincaré value of -2π does not belong to a singular point. It is, however, a theoretically possible value. A poincaré index of -2π would require friction ridges to shape a very unnatural *diamond* shape around a given point, see Figure 6.7. This does not occur in a normal fingerprint image; however, it has been seen to occur in highly obliterated or unclear areas.

After calculating the Poincaré index for all pixels in the fingerprint image, the Poincaré matrix, $P_b(x, y)$, is binarised accordingly:

$$P_b(x,y) = \begin{cases} 1, & \text{if } P(x,y) \in \{\pm\pi, \pm 2\pi\} \\ 0, & \text{otherwise} \end{cases} \tag{6.9}$$

The resulting binarised Poincaré image will generally have a small cluster of one to four adjacent pixels with high values in the singular regions. However, noisy or low quality areas in unaltered images may lead to the detection of additional false singular points.

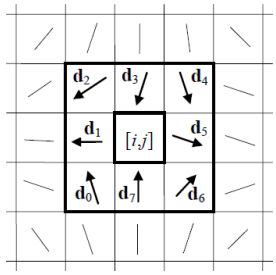

(a) Diamond (-360°)

Figure 6.7: Poincaré index of -360 would require orientations in a special *diamond* shape.

The unnatural flow of friction ridges in altered fingerprints will generally result in a higher detection of false singular points. Figure 6.8 shows the resulting binarised Poincaré image, P_b, of two unaltered fingerprints. Figure 6.8d illustrates the problem with poor quality fingerprint images. Figure 6.9 shows P_b of altered images.

An observation can be made on the spurious false singularities found in both altered and unaltered fingerprints that can further strengthen the analysis of singularities and help detect if a fingerprint has been altered or not. As already stated, false minutia is detected in areas of low quality. However, scarred areas which are connected to friction ridges with regular ridge-valley patterns also contribute to the detection of false singular points.

In the following section Gabor filters will be used to determine quality measures of the friction ridges. The basic idea is to highlight *singular points* in good quality areas.

6.3 Gabor Filters

The goal is to determine the clarity of friction ridges in a fingerprint so that found singularities can be classified based on the quality score of their position. Gabor filters will be used to measure the quality of friction ridges. Gabor filters are bandpass filters that have both frequency and orientation properties; they can therefore be constructed to present friction ridge frequency and orientation.

Shen *et al* [SKK01] proposed a block-wise approach using Gabor filters to determine the quality of friction ridges. A global quality measure based on Gabor

(a) Original **(b)** P_b **(c)** Original **(d)** P_b

Figure 6.8: Singular point detection of unaltered fingerprints. (a) Fingerprint image [CMM+04], (b) its corresponding binarised Poincaré image with highlighted readings, (c) Poor quality fingerprint image [CMM+04], (d) its corresponding binarised Poincaré image. Low quality images will result in spurious false singularities.

filter responses was proposed by Olsen *et al* [OXB12]. The latter approach will be used in this thesis adopting the suggested filter bank size from the prior.

The first step is to convolve the fingerprint image, I, with a two-dimensional Gaussian with $\sigma = 1$. The convolution is subtracted from the original image to give $\bar{I}$ which is a high-pass filtered image.

The quality of the ridge-valley structure of the friction ridges is found by convolving the fingerprint image, $\bar{I}$, with two-dimensional Gabor filters in n orientations ($n = 8$). The orientations θ are computed:

$$\theta = \pi \frac{k-1}{n}, \quad k = 1, .., n \tag{6.10}$$

Hamamoto *et al* [HUW+98] define the general form of a complex two-dimensional Gabor filter in the spatial domain as:

$$h(x, y, \theta_k, f, \sigma_x, \sigma_y) = exp(-\frac{1}{2}(\frac{x_{\theta_k}^2}{\sigma_x^2} + \frac{y_{\theta_k}^2}{\sigma_y^2}))exp(j2\pi f x_{\theta_k}), \quad k = 1, .., n \tag{6.11}$$

where

n is the number of orientations used in the filter bank
$x_{\theta_k} = x \sin\theta_k + y \cos\theta_k$,
$y_{\theta_k} = x \cos\theta_k - y \sin\theta_k$,
f is the frequency of the sinusoidal plane wave along the orientation θ_k,
σ_x and σ_y are the parameters of the Gaussian window.

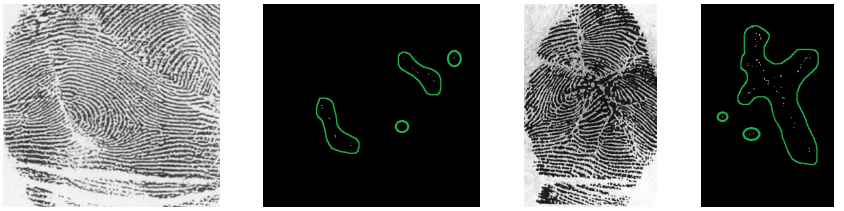

(a) Original **(b)** P_b **(c)** Original **(d)** P_b

Figure 6.9: Singular point detection of altered fingerprints. (a) Distorted fingerprint [Wer98], (b) its corresponding binarised Poincaré image with highlighted readings, (c) Heavily damaged fingertip [Sam01], (d) its corresponding binarised Poincaré image.

The filter frequency, f, is set to 0.1 as the average inter-ridge distance (corresponding to the wavelength) is approximately 10 pixels in a 500 dpi fingerprint image [JPHP00]. The standard deviation of the Gaussian envelope along the x and y axes are set as $\sigma_x = \sigma_y = 6.0$.

The magnitude of the responses is convolved with a two-dimensional Gaussian with $\sigma = 4$ to smoothen the magnitudes. Areas containing clear ridge-valley structures will have a strong response from one or more of the filter orientations, see Figure 6.10 while low quality areas will have low responses.

A pixel-wise standard deviation of the bank of Gabor responses is calculated, G_{std}.

The resulting Gabor quality matrix, G_{std}, is transformed to lie in the interval $[0, 1]$ by:

$$Q_G(x, y) = \begin{cases} G_{std}(x, y)/T, & \text{if } G_{std}(x, y) \leq T \\ 1, & \text{otherwise} \end{cases} \tag{6.12}$$

where T is a given threshold ($T = 0.01$). The threshold is determined empirically.

6.4 Density Map

The quality metrics matrix, Q_G, are factors that determine the quality of friction ridges in each pixel. The quality score is defined in the interval $[0, 1]$ where 1 is the best quality.

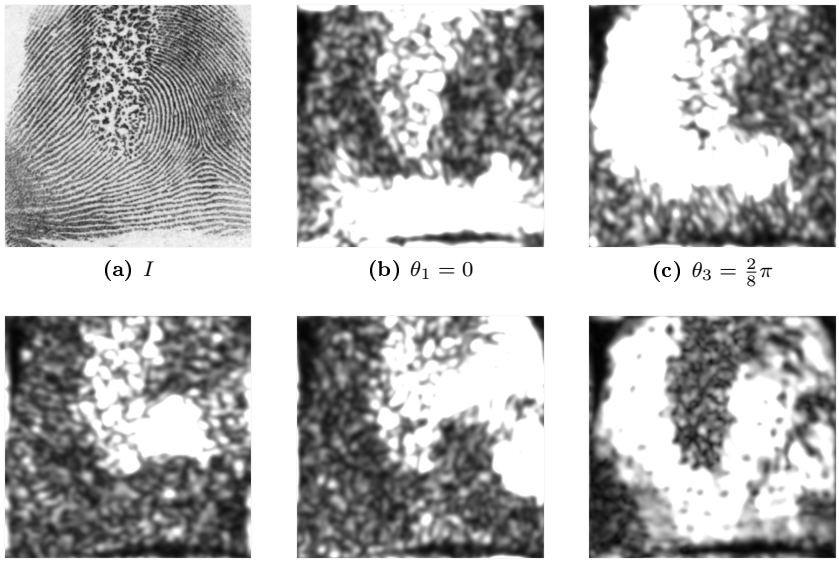

(a) I (b) $\theta_1 = 0$ (c) $\theta_3 = \frac{2}{8}\pi$

(d) $\theta_5 = \frac{4}{8}\pi$ (e) $\theta_7 = \frac{6}{8}\pi$ (f) Q_G

Figure 6.10: Gabor filter responses of an obliterated fingerprint. (a) input image [YFJR09], (b)–(e) absolute values of Gabor filter responses in different orientations after Gaussian smoothening and (f) standard deviation of the Gabor responses with different orientations.

An initial density map, P_d, is created from combining the Poincaré matrix, $P_b(x, y)$, and the normalised Gabor quality matrix, Q_G, by multiplication:

$$P_d(x, y) = P_b(x, y) \cdot Q_G(x, y) \tag{6.13}$$

P_d is a density map where singularities positioned within clear areas receive a higher value than singularities in poor quality areas.

Similar to the previous minutia distribution analysis, the final density map, SP_d, is constructed by using the Parzen window method with uniform kernel function and smoothed using a low-pass Gaussian filter. To feed the information into a SVM, a feature vector is extracted from the density map using the same method as in the minutia distribution analysis.

Figures 6.11 and 6.12 show examples of the final density maps of unaltered and altered fingerprints, respectively. Notice that the altered fingerprints have a higher density of singularities than the unaltered in the final density maps.

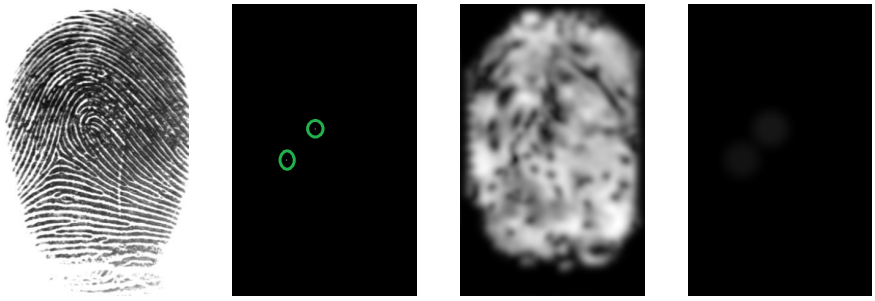

(a) Original **(b)** P_b **(c)** Q_G **(d)** SP_d

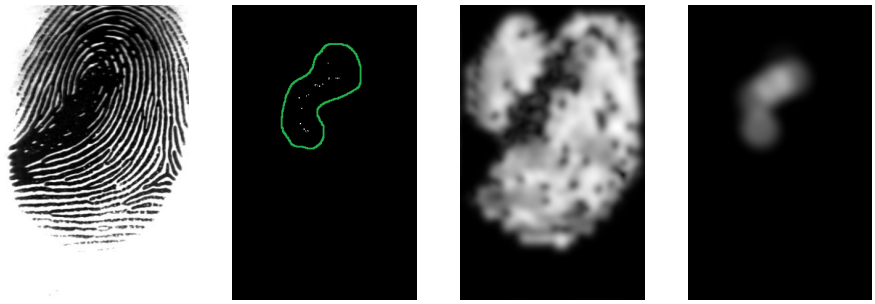

(e) Original **(f)** P_b **(g)** Q_G **(h)** SP_d

Figure 6.11: Singular point density analysis of unaltered fingerprints. (a) input image, (b) its corresponding binarised Poincaré image with highlighted readings, (c) quality measurement of the friction ridges, (d) the final singular point density map. (e)–(g) show the same as (a)–(d) but with a lower quality image. Source: (a), (e) [CMM+04].

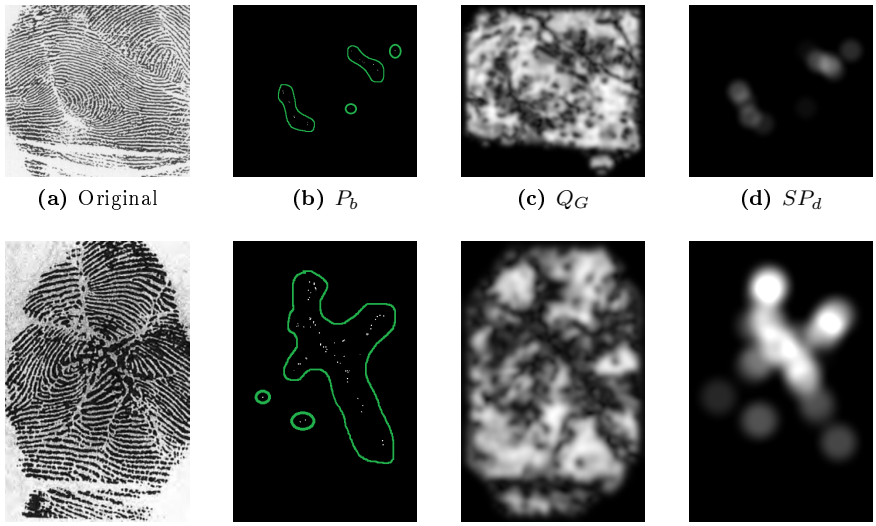

(a) Original **(b)** P_b **(c)** Q_G **(d)** SP_d

(e) Original **(f)** P_b **(g)** Q_G **(h)** SP_d

Figure 6.12: Singular point density analysis of altered fingerprints. (a) input image, (b) its corresponding binarised Poincaré image with highlighted readings, (c) quality measurement of the friction ridges, (d) the final singular point density map. (e)–(g) show the same as (a)–(d) with a heavily damaged fingertip. Source: (a) [Wer98], (e) [Sam01].

6.5 Summary

Uncertainties in the orientation field are introduced around altered areas of a fingerprint. The disorder of pixel-wise orientations in scarred and obliterated areas share similar characteristics to that of singular regions.

An analysis based on the distribution and density of *singular regions* is conducted using the Poincaré index to locate singular point candidates. Altered images will generally have a distribution of singular point candidates which differs from natural fingerprints.

Gabor filters are used to determine a fingerprint quality measurement of the clarity of friction ridges. This is used to slightly reduce the effect of spurious singular regions found in areas which are heavily obliterated. Singularities found in unclear areas will have a weaker amplitude in the final density image.

Chapter 7

Minutia Orientation Analysis

Yoon *et al* [YFJ12] have demonstrated that the minutia distribution of altered fingerprints often differs from that of a natural fingerprint. The main reason being that scars and obliterated areas will provide additional spurious minutia due to ridge discontinuity.

The Minutia Orientation Analysis (MOA) takes advantage of the excessive number of minutia that appear due to alteration. Instead of relying on the actual distribution of minutia as the MDA does, properties of minutia in local areas will be analysed to try to determine if a fingerprint has been altered or not.

7.1 Pre-Analysis

Altered fingerprints have an unnatural orientation flow. The Orientation Field Analysis (OFA) proposed by Yoon *et al* [YFJ12] takes a global approach to determine these inconsistencies in the orientation field. Likewise, the MOA showed that minutia distribution of altered fingerprints often differs from that of natural fingerprints.

Scars will produce broken ridges which will contribute to some of the additional minutiae that is extracted from altered fingerprints. Figure 7.1 shows an example of a z-cut alteration where a relatively large portion of minutiae is concentrated around the scarred areas.

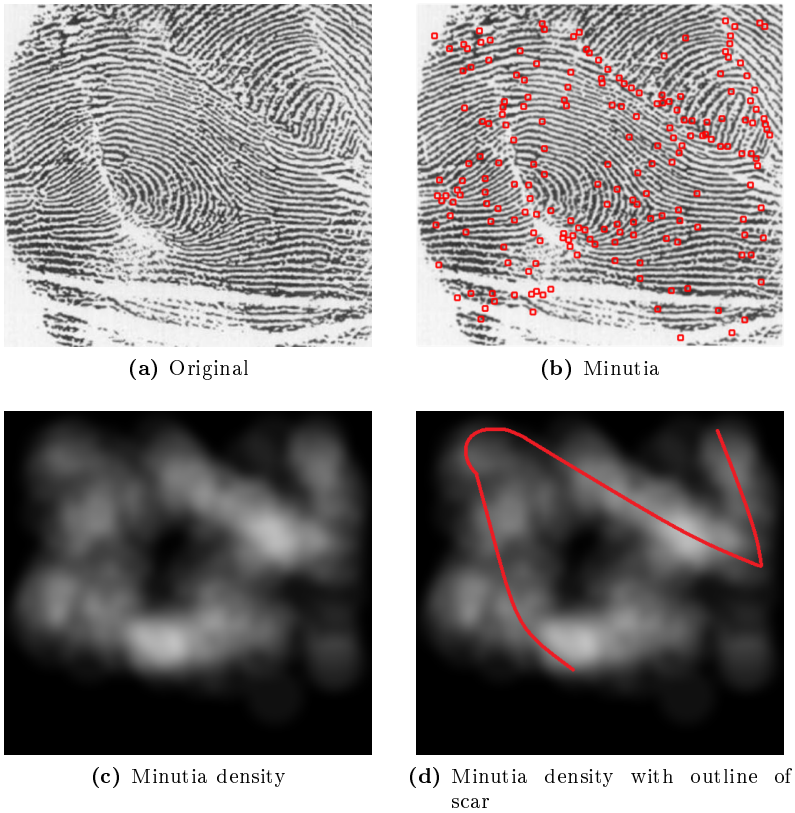

(a) Original **(b)** Minutia

(c) Minutia density **(d)** Minutia density with outline of scar

Figure 7.1: Scars will typically have a higher concentration of minutiae. Source: (a) [Wer98].

Fingerprints with transplanted skin will typically have sudden changes in the orientation of friction ridges in some areas along the scars. This is caused by the joining of skin with different friction ridge patterns which are separated by the scar. Friction ridges on each side of scars caused by small cuts will have somewhat continuous flowing orientations.

The following method that will be proposed will try to analyse and identify unnatural orientation changes in the friction ridges by analysing the detected minutiae. The idea is to register a metric for each minutia point which describes

the change in orientation in its surroundings.

There are multiple options that can be considered. Two simple approaches based on analysing orientations in a certain radius, r, from the minutia could be:

1. Using a rotating line. A circle of radius r is considered around each minutia point. Using the computed orientation field, the maximum difference of orientation between a series of orientation pairs on opposite sides of the circle around the minutia point can be found based on Figure 7.2. Here, steps of $\frac{\pi}{4}$ are used to find a set of 8 points around the minutia point. The minutia is assigned the maximum difference in orientation of the points on opposite sides of the minutia.

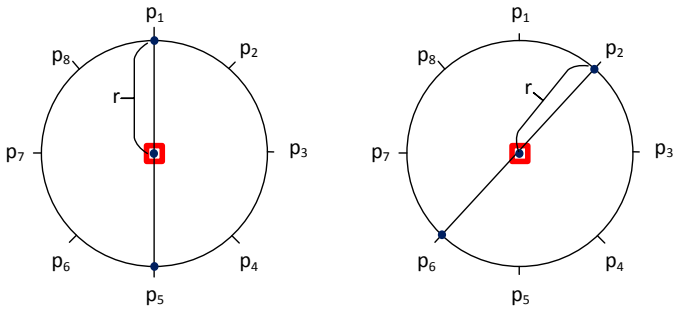

Figure 7.2: Differences in orientations can be measured based on points in a certain distance, r, from the minutia. A line is rotated clockwise in steps of $\frac{\pi}{4}$ around the minutia center. (a) First the orientation difference between points p_1 and p_5 are found, (b) the line is rotated and the difference between points p_2 and p_6 are found, and so on. The minutia is assigned the maximum orientation difference of the four measurements.

2. Based on minutia direction. The minutia extractor assigns a direction to every minutiae, normally in the range $[0, 2\pi)$, pointing towards the current friction ridge that it belongs to. Instead of analysing multiple points around a circumference with radius r around the minutia, only the point in the given direction of the minutia and on the opposite side are measured like earlier. The minutia is assigned the orientation difference of these two points. This can be seen in Figure 7.3.

The problem with both of the above mentioned approaches is that minutia close

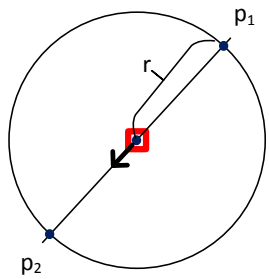

Figure 7.3: Differences in orientations can be measured based on points in a certain distance, r, from the minutia. Points are found by the actual orientation of the minutia. The minutia is assigned the orientation difference of points p_1 and p_2.

to high curvature regions, such as singularities, will be assigned high values. The second approach is an improvement since it takes into account the actual direction of the minutia.

Instead a simple method is proposed based on comparing neighbouring minutia, that are closer than a given radius. To compare neighbouring minutiae, it is desired that minutia are found on both sides of scars in order to analyse changes. The problem comparing minutia, is that minutia extractors generally do a lot of analyses of candidate minutiae in order to remove false minutiae. Even though the density of minutiae is higher along scars, the minutia extractor does a good job in limiting minutia with conflicting orientations.

Before further introducing the proposed method, a basic understanding of the minutia extractor is required in order to improve the feature extraction algorithm for this specific analysis.

7.2 Minutia Extractor

The minutia extractor, *Mindtct*, that has been used in this project has six main processes [WGT+] which here have been categorised into three smaller categories: preprocessing, feature extraction and minutia analyses. An overview of these processes can be seen in Figure 7.4. The following sections will briefly describe these categories. The focus will be on the processes that specifically can have an influence on altered images.

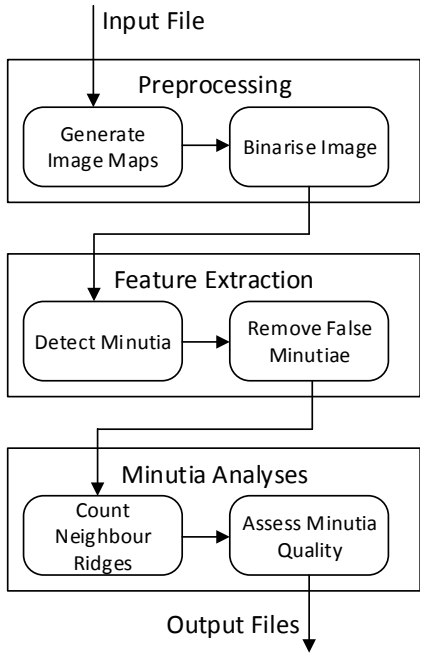

Figure 7.4: Process of NIST's minutia extractor Mindtct.

7.2.1 Preprocessing

The preprocessing pipeline of the minutia extractor has two main purposes: to analyse the quality of the fingerprint and prepare it for feature extraction. Specifically, the quality measurements are made by generating multiple image maps. Subsequently the fingerprint is binarised where each pixel in the image is assigned either a black or white pixel denoting ridges and valleys, respectively.

7.2.1.1 Image Maps

The input fingerprint image is analysed in order to determine poor quality areas in the image. The following characteristics are calculated:

- Orientation Field. A block-wise orientation field is constructed using a filter-bank based approach in the frequency domain. Each block is incrementally rotated $\pi\frac{k-1}{16}$, for $k = 1, .., 16$ and thereafter analysed by

convolving a vector of the block's row sums with different waveforms of increasing frequency. Each block is assigned the orientation that best fits one of the waveform filters; no orientation can be assigned if no dominant ridge flow can be determined.

- Low Contrast Map. This is basically a segmentation mask (see 5.2) based on the image contrast. No morphological operations are performed on this segmentation mask. Minutia will only be detected in the found ROI.

- Low Flow Map. Is basically a map marking which blocks in the orientation field do not currently have a valid direction; these blocks are marked as having low quality and minutia extracted from these blocks will be seen as less reliable.

- High Curve Map. A map is constructed that marks blocks in areas of high curvature, e.g. around singular points of the fingerprint. If minutia are extracted from these blocks they will also be assigned a lower quality.

- Quality Map. The low contrast map, low flow map and high curve map are combined to construct a single quality map.

Once the above mentioned maps have been constructed, the orientation field is further modified. Analysis based on neighbouring blocks is performed to: smoothen orientations, interpolate invalid direction blocks with neighbours and even removing additional directions that are inconsistent with surrounding blocks.

Heavily obliterated areas which have significantly unclear ridges might end in the low contrast map – minutia will therefore not be found in these areas. The areas of interest are especially scarred regions caused by alterations which generally have sufficiently high contrast. Scarred regions have a high risk of being in either the low flow map or high curve map. This happens if the orientation is unclear or if the alteration causes sudden changes in the friction ridge orientation, respectively.

7.2.1.2 Binarise Image

The second step of the preprocessing is preparing the actual fingerprint image for minutia extraction. A binarised image is constructed to represent the fingerprint image. Each pixel in the image is assigned a binary value based on attributes of the surrounding pixels of the original image together with the friction ridge orientation.

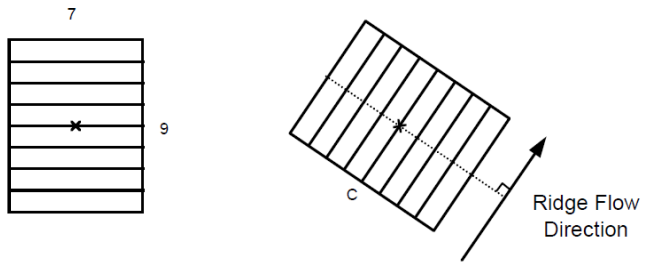

Figure 7.5: Rotated block with processed pixel in centre used to binarise fingerprint image. Source: [WGT+]

A block of size 7×9 is constructed around the pixel that is being processed, i.e. a border of 3 columns and 4 rows surrounding the processed image. The block is rotated so that the rows align with the orientation of the pixel in the orientation field, see Figure 7.5. The intensities (grey values) are accumulated for each row of the block, forming a vector of row sums.

The binary value to be assigned to the center pixel is determined by multiplying the center row sum by the number of rows in the grid and comparing this value to the accumulated grayscale intensities within the entire grid. If the multiplied center row sum is less than the grid's total intensity, then the center pixel is set to black; otherwise, it is set to white.

If the accumulated sum of the center row is smaller than the average row sum, the value is set to 0 (black); otherwise it is set to 1 (white). The formula for the binarised image, B, is the following:

$$\forall x \in \{1..R\}, y \in \{1..C\} : B(x,y) = \begin{cases} 0 & \text{if } R_b \cdot \mathbf{r}_{x,y}[\frac{R_b-1}{2}] < \sum_{i=1}^{R_b} \mathbf{r}_{x,y}[i], \\ 1 & otherwise \end{cases} \quad (7.1)$$

where $R_b = 9$ and $\mathbf{r}_{x,y}$ is the vector of row sums belonging to pixel (x, y).

7.2.2 Feature Extraction

The image is now ready for feature extraction. The minutia extractor first tries to identify possible minutia candidates. Thereafter the candidate list will be further analysed in order to remove false minutia.

7.2.2.1 Detect Minutia

Minutia are detected by identifying localized pixel patterns in the binary image. Even though there are many common types of minutia, see Figure 7.6, the feature extraction algorithm takes advantage of the fact that the types can basically be narrowed down to two: ridge ending and bifurcation. Every minutia point can fall into one of these two, as an example a *spur* is a combination of a bifurcation and a ridge ending while an *independent ridge* consists of two ridge endings.

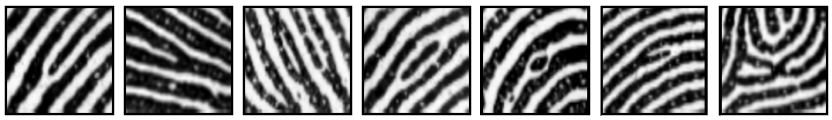

Figure 7.6: Common types of minutia. (a) ridge ending, (b) bifurcation, (c) lake, (d) independent ridge, (e) island or point, (f) spur, (g) crossover. Source: [MMJP09]

A series of different sized patterns are constructed that represent ridge endings and bifurcation. The binarised image is scanned looking for sequences that match the given patterns, see Figure 7.7. Note that the patterns grow by inserting multiple instances of the centre row into the patterns. The image is scanned vertically and horizontally; the horizontal scan rotates the patterns 90° clockwise. Each sequence that matches one of the given patterns is added to the candidate list.

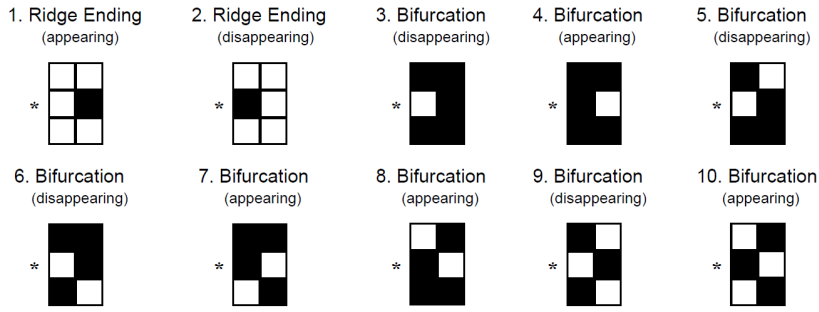

Figure 7.7: Pixel patterns used to detect minutiae. The * represents center rows that can be repeated one or more times. Source: [WGT+]

7.2.2.2 Remove False Minutiae

The pixel pattern approach that is used to find minutia is an exhaustive and greedy algorithm which will detect most true minutia, but also include many false minutia in the candidate list. The feature extractor therefore does a thorough analyses of the minutia in the candidate list in order to remove the false candidates.

A simplified description of the different steps taken in order to remove false minutia will be given below. The NBIS documentation [WGT+] and the source code of *Mindtct* [WGTW12] can be referenced for a more precise and detailed description. The remove process does the following:

- Remove islands and lakes. Islands can be formed by ridge ending fragments and spurious ink marks while lakes are small holes or voids within ridges. A pair of candidate minutia will be detected at each end of islands and lakes. If two minutiae are found to be closer than a given threshold (16 pixels) with directions that are nearly opposite, the pair of minutiae are removed from the candidate list.
- Remove islands on holes in the binary image defined by a single point. Smaller islands or lakes might be represented by only one single minutia point. If a minutia point belongs to a ridge or valley area with a perimeter length ≤ 15 pixels, then it is removed from the candidate list.
- Remove minutiae that point sufficiently close to a block with invalid direction. If a minutia point is closer than 4 pixels – in the direction it is pointing – of a block containing an undefined ridge flow direction, then it is removed.
- Remove minutiae that are sufficiently close to a block with invalid direction. If minutia are close to blocks with undefined directions, which also have additional neighbours with invalid direction, the minutia is removed. The idea is that the candidate minutia is either close to the border of the fingerprint or close to a larger area of poor quality.
- Remove or adjust minutiae that reside on the side of a ridge or valley. Some candidate minutiae might not be located at ridge or valley endings, but instead on the side of ridges or valleys caused by noisy or uneven ridge/valley areas. Using rotated blocks a closer analysis is done to determined if the minutia is located on a *well formed* ridge/valley ending; which is at the bottom of a bowl-shaped rotated contour.
- Remove minutiae that form a hook on the side of a ridge or valley. Hooks (see 7.6) will typically produce a pair of minutiae where one is a bifurcation

and the other is a ridge ending. If two such minutia are close to each other (within 16 pixels), on the same ridge or valley, and have directions nearly opposite each other, then both minutiae points are removed from the candidate list.

- Remove minutiae that are on opposite sides of a broken ridge. Ridges can be broken by such things as flexion ridges or scars. Again, discontinuity in ridges or valleys, will produce a pair of minutiae. If two minutia with almost opposite directions are closer than 8 pixels then they are removed, provided that the direction between the two minutia also is similar to one of the minutia directions.

- Remove minutiae that have *irregularly* shaped ridges or valleys. Tests are conducted to ensure that the structure enveloping a ridge or valley ending is relatively Y-shaped and not too wide.

- Remove minutiae that form long, narrow, ridges or valleys in the *unreliable* regions in the binary image. Similar to the prior process: minutia are removed that belong to ridge or valley structures that are too narrow.

7.2.3 Minutia Analyses

The feature extractor prepares output files in multiple formats and with additional information intended for miscellaneous fingerprint comparison algorithms. The final category of the feature extraction algorithm is to perform additional analyses of the minutia in order to provide further attributes and information to the subsequent minutia comparator.

Additional information from the feature extractor will not be used in the upcoming alteration detection algorithm and will therefore only be mentioned very briefly. The two main processes are:

- Count neighbour ridges. Some minutia comparing algorithms use topological correspondence, such as minutia direction and ridge counts between neighbouring minutia, to compare fingerprints.

- Assess minutia quality. Quality measurements are produced for each detected minutia; these are based on the quality map combined with pixel intensity statistics.

7.3 Modified Minutia Extractor

Based on the above dissection of the minutia extractor small modifications are made to the source in order to provide additional minutiae in strategic places. It is very important that the extractor still filters out minutiae; leaving out the whole filtering process would result in an excessive amount of minutiae. This would lead to large areas around singularities being identified as having unnatural changes in the flow of friction ridges based on the high curvatures.

Modifications are the following:

- Islands and Lakes. A pair of candidate minutia will be detected at each end of islands and lakes. If two minutiae are found to be closer than a given threshold (16 pixels) with a minimum direction angle $\geq 123.75°$, then the pair of minutiae are removed from the candidate list. An illustration of this is shown in Figure 7.8.

  The modified version increases the threshold of the direction angle to $157.5°$. This will give a larger amount of minutiae belonging to small islands and lakes.

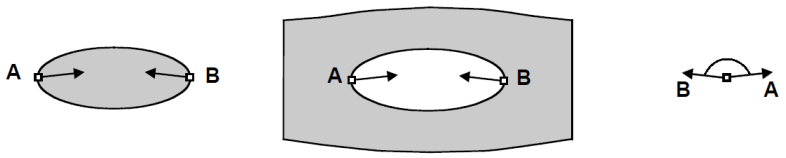

(a) Island **(b)** Lake **(c)** Direction angle

Figure 7.8: The minimum direction angle between a pair of minutiae points is used to determine if candidate minutiae are removed or not.

- Hooks. Scarred regions will produce hooks that protrude off the side of ridges. It would therefore seem obvious to keep candidate minutia belonging to hooks in the modified minutia extractor. The problem with hooks is that they have directions which do not correspond to the actual ridge flow in the corresponding area, see Figure 7.9. Leaving minutiae belonging to hooks will increase the inconsistency of minutiae directions in unaltered regions of the fingerprint also. This is therefore unmodified in the current solution.

- Discontinuities. Minutiae belonging to discontinuities (see Figure 7.10) in ridges or valleys are removed in the standard feature extractor. Criteria

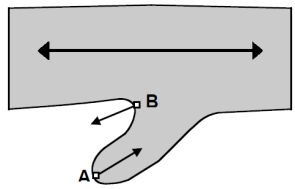

Figure 7.9: Minutiae belonging to hooks have directions that differ from the friction ridge orientation.

is based on a combination of minutia distance, the difference of the directional angles between them and the direction of a line joining the two minutiae points.

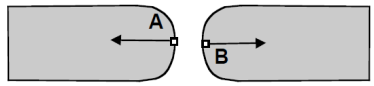

Figure 7.10: Discontinuities in ridges or valleys have a pair of minutiae points in opposite directions.

Friction ridges on opposing side of scars can be considered as discontinuities. The modified feature extractor leaves out this check and does therefore not remove minutiae on the basis of discontinuities. Discontinuities in unaltered regions will not have a great impact on the analysis of minutia orientations since they generally are consistent with the local friction ridge orientation.

- Unreliable orientation. Alterations with a sufficient amount of friction ridges will reside in a region with an orientation – it will be unreliable – and will generally belong to the ROI of the fingerprint. Minutiae in these areas will typically have a lower quality score. Checks dealing with unreliable/invalid orientations are therefore unmodified in the feature extractor.

- Irregular shaped ridges/valleys. The checks that test if ridges are to wide or too narrow do not greatly affect the minutiae points around scars and obliterated regions and will therefore be unmodified in the feature extractor.

Only a couple of small modifications are done to the feature extractor. To summarise the above, only the process that removes islands and lakes has been modified while the process that checks for discontinuities has been removed.

7.4 Algorithm

A modified minutia extractor is prepared which gives more *false* minutiae. The feature extractor will provide additional minutia around ridge discontinuities and around spurious islands and lakes. These friction ridge features are common around mutilated areas of a fingerprint.

The Minutia Orientation Analysis (MOA) is a relatively simple algorithm which analyses local orientation differences of minutiae. Each minutia point compares its orientation with every surrounding minutiae within a given radius, see Figure 7.11. The largest orientation difference is registered and saved in a *orientation difference* map. A density map is then constructed from the orientation difference map.

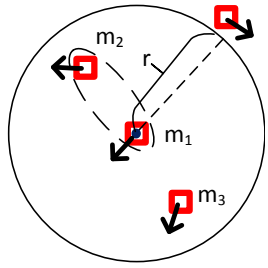

Figure 7.11: Each minutia point finds the minutia with the largest orientation difference from its own within a given radius, r. Minutia point m_1 is being processed. Only minutia within the given radius are considered. Minutia point m_2 differs most from m_1; the minutia which is being processed is assigned the orientation difference of these two points.

Descriptions on how the orientation difference and orientation density maps are created is described below.

7.4.1 Orientation Difference Map

A function is introduced $\phi(\mathbf{u}, \mathbf{v}, r)$ which gives 1 if the distance between points $\mathbf{u}$ and $\mathbf{v}$ is less than a given radius (distance), r, and 0 otherwise:

$$\phi(\mathbf{u}, \mathbf{v}, r) = \begin{cases} 1 & \frac{|\mathbf{u}-\mathbf{v}|}{r} < 1, \\ 0 & otherwise \end{cases} \tag{7.2}$$

Minutia directions are in the range $[0, 2\pi)$. The directions are transformed to lie in the interval $[0, \pi)$, using modulo π, such as they now are orientations. The difference, $d(\theta_i, \theta_j)$, between two minutia orientations, θ_i and θ_j, is given as:

$$d(\theta_i, \theta_j) = \min(|\theta_i - \theta_j|, \pi - |\theta_i - \theta_j|) \tag{7.3}$$

Let $\mathbf{S_m}$ be the set of minutiae of the fingerprint containing the minutia's position and orientation, i.e.,

$$\mathbf{S_m} = \{(\mathbf{x}, \theta) \quad | \quad \mathbf{x} = (x, y) \text{ is the position and } \theta \text{ is the orientation of minutia}\}. \tag{7.4}$$

A set, $\mathbf{S_{diff}}$, containing the position of each minutia together with the largest orientation difference is given as:

$$\mathbf{S_{diff}} = \{(\mathbf{x}, \theta_{max}) \quad | \quad (\mathbf{x}, \theta) \in \mathbf{S_m} \wedge \theta_{max} = \text{Max}(\mathbf{x}, \theta, r, \mathbf{S_m})\}, \tag{7.5}$$

where $r = 30$ and $\text{Max}(\mathbf{x}, \theta, r, \mathbf{S_m})$ returns the largest orientation difference, a, between θ and any minutia within the radius r by equation (7.6).

$$\forall b \in \{\phi(\mathbf{x}, \mathbf{x_0}, r) \cdot d(\theta, \theta_0) \quad | \quad (\mathbf{x_0}, \theta_0) \in \mathbf{S_m}\} : (b \leq a) \tag{7.6}$$

The initial minutia orientation difference map, $M'_{diff}(x, y)$, is initiated by zeroes in the size of the fingerprint image. The minutia difference values, $\mathbf{S_{diff}}$, are plotted into M'_{diff} such that the location of each minutia is assigned the corresponding minutia orientation difference.

The values of $M'_{diff}(x, y)$ are transformed to lie in the interval $[0, 1]$ by

$$M_{diff}(x, y) = \begin{cases} M'_{diff}(x, y)/T, & \text{if } M'_{diff}(x, y) \leq T, \\ 1, & \text{otherwise} \end{cases} \tag{7.7}$$

where T is a predetermined threshold (T is set to $\pi/4$).

M_{diff} is basically an image where each pixel $M_{diff}(x, y)$ contains a normalised orientation difference of the minutia centred at (x, y). If no minutia is in (x, y) then the value is 0.

7.4.2 Density Map

The final density map is computed using the same methods as the other density maps:

1. An initial density map, M'_{dens}, is constructed by

$$M'_{dens}(\mathbf{x}) = \sum_{\mathbf{x_0} \in M_{diff}} K_r(\mathbf{x} - \mathbf{x_0}) \tag{7.8}$$

where $K_r(\mathbf{x} - \mathbf{x_0})$ is a uniform kernel function centred at $\mathbf{x_0}$ with a radius r (r is set to 30 pixels).

2. Smoothening. The initial density map, M'_{dens}, is smoothed by a low-pass Gaussian filter of size 30×30 with a standard deviation of 10 pixels.

3. Normalisation. The values of $M'_{dens}(\mathbf{x})$ are transformed to lie in the interval $[0, 1]$ by

$$M_{dens}(x, y) = \begin{cases} M'_{dens}(x, y)/T, & \text{if } M'_{dens}(x, y) \leq T, \\ 1, & \text{otherwise} \end{cases} \tag{7.9}$$

where T is a predetermined threshold (T is set to 6.9).

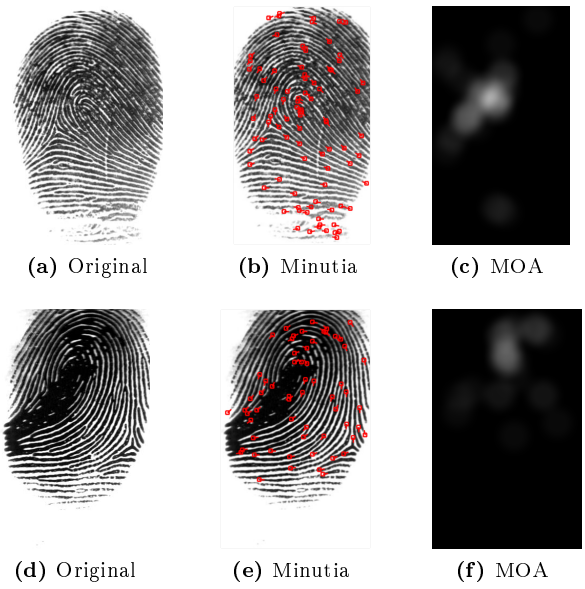

(a) Original **(b)** Minutia **(c)** MOA

(d) Original **(e)** Minutia **(f)** MOA

Figure 7.12: MOA of two unaltered fingerprints. Minutia points generally share similar orientations to their neighbouring minutia. Singular regions will introduce some variations; the MOA will therefore have higher amplitudes around singular regions. Source: (a), (d) [CMM+04].

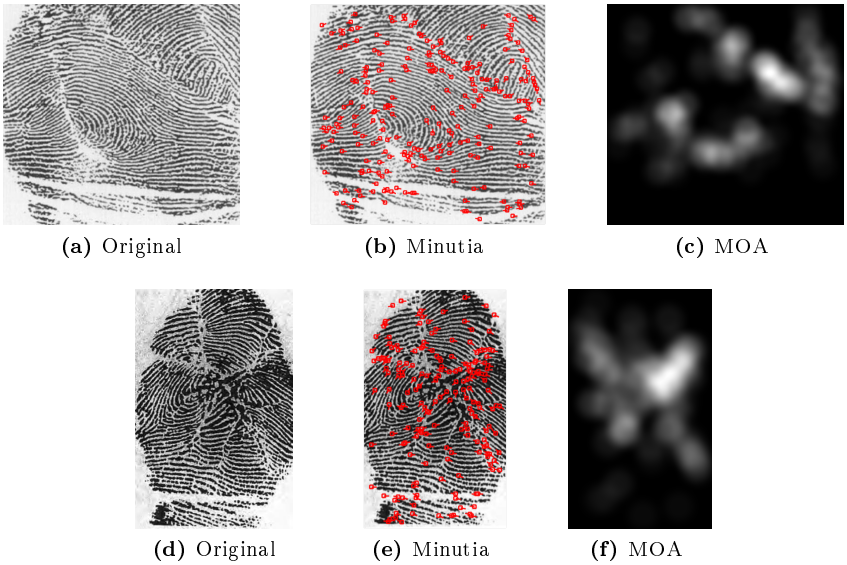

(a) Original **(b)** Minutia **(c)** MOA

(d) Original **(e)** Minutia **(f)** MOA

Figure 7.13: MOA of two altered fingerprints. Regions around scars with irregular orientations will add additional high amplitudes to the MOA density map. Source: (a) [Wer98], (d) [Sam01].

Figures 7.12 and 7.13 show the resulting density map of the MOA. A natural fingerprint will generally only have small peaks around singular regions. The additional minutia around scars and obliterated areas with conflicting orientations in altered fingerprint images will produce areas with higher amplitudes such that the distribution of the density image will differ from an unaltered fingerprint image.

7.5 Summary

Minutiae are points of bifurcation or termination of the friction ridges. Altered fingerprints will introduce additional discontinuities in the friction ridges which will result in a distinct distribution of minutiae that differs from unaltered fingerprint images.

The MOA identifies discrepancies by analysing and comparing attributes of neighbouring minutia. The analysis finds the largest orientation differences of minutia within a given radius and plots them in a density map.

To increase the efficiency of this analysis a modification has been done to the filtering process of minutiae candidates in the minutia extractor. The modification introduces additional minutiae with conflicting orientations around scars.

Chapter 8

Results and Evalutaion

The previous chapters have described a proposed method for detecting altered fingerprints along with an existing state-of-the-art method proposed by Yoon *et al* [YFJ12]. This chapter will describe some experimental results and give a brief evaluation of the proposed method.

8.1 Metrics

There are four metrics defined for evaluating the *altered presentation characteristics* detection rate [ISO12]:

- True Altered Detection Rate (TADR) is the proportion of altered presentation characteristics correctly classified as being altered.
- True Non-Altered Detection Rate (TNADR) is the proportion of non-altered presentation characteristics correctly classified as being non-altered.
- False Altered Detection Rate (FADR) is the proportion of non-altered presentation characteristics incorrectly classified as being altered.
- False Non-Altered Detection Rate (FNADR) is the proportion of altered presentation characteristics incorrectly classified as being non-altered.

Generally, it must be considered impossible to correctly classify the altered presentation characteristics of every fingerprint image. The desirable results are to have a high TADR together with a low FNADR, i.e. that many altered fingerprints are detected as altered while only a few unaltered fingerprints are detected as altered.

8.2 Experimental Setup

Before the actual results are presented, a description of the testing environment will be given.

8.2.1 Fingerprint Database

Data sensitivity issues limit the amount of publicly available datasets with altered fingerprints. Fingerprints with alterations are defined as sensitive personal data since it contains information about individuals trying to hide their identity for reasons such as criminal offences. Even though fingerprints are altered, they may still hold enough information for a positive identification.

Generally, access can only be attained to genuine altered fingerprints obtained by government officials by consent of the individual. In special cases of substantial public interest, permission can sometimes be granted to process such data in a controlled environment. Access to a database containing genuine altered fingerprints obtained by government officials is therefore considered an almost impossible task.

For the experimental testing images have been collected from multiple public sources and also obtained from other research centres. The majority of altered fingerprints are collected for dermatological purposes and contain fingertips that have unintentional alterations caused by diseases or injuries. Many of the distorted images are caused by surgical procedures, e.g. scars or transplantations from medical corrections of mutilated areas. The final database composition is comprised of the following:

- Brno [Brn13]. A collection of fingerprints containing a wide variety of dermatological diseases. The database is a property of the Faculty of Information Technology at Brno University of Technology and the research group STRaDe in collaboration with dermatologists from FN Olomouc. Skin diseases can have a great influence on the fingerprint pattern. Many

fingerprints share characteristics similar to altered fingertips, especially belonging to the obliterated classification. Some images with only minor alterations have been classified as unaltered prior to testing, since they are considered to contain enough information for a positive comparison decision by an AFIS.

- FVC 2004 [CMM+04]. The public fingerprint database collected for the Fingerprint Verification Competition 2004 (FVC 2004). Images from database DB1 (set A) were used - all images are unaltered.
- GUC-100 [GUC09]. An *in-house* database from Gjøvik University College (GUC) in Norway. A few images contained dermatological diseases with unnatural ridge flow which were of special interest.
- Samischenko [Sam01]. The book *Atlas of the Unusual Papilla Patterns* by S.S. Samischenko contains a large collection of fingerprint images with unusual fingerprint patterns together with some natural. The database contains fingerprints from fingers altered by burns, acid burns, transplantation, miscellaneous injuries and diseases.
- Literature sources. An assortment of images, primarily altered, where gathered from miscellaneous literature sources, such as books, presentations and articles.

It is difficult to obtain data with a reliable ground truth, e.g. all fingerprint images with dermatological diseases are not necessarily classified as altered. Images have therefore been manually sorted and classified as altered or unaltered prior to any research on the detection methods. The ground truths were never changed.

Since many of the altered fingerprint images are from literature sources of poor quality, a large amount of the available images are deemed unsuited for the actual testing since they will produce unrealistic results most likely in the favour of the proposed method. The final dataset used for testing contains a filtered version of the collected databases based on image quality.

The final filtered dataset used for testing contains 116 good and varied images of altered fingerprints. Given the difficulty of gathering a variety of altered images with an adequate quality, the dataset must be considered to be of a high standard. Apart from the large government dataset used by Yoon *et al* [YFJ12, YZJ12], most other research is either done on a very limited dataset, e.g. [PL12], or on synthetic or simulated database, e.g. [FJR09], [TPVR12] and [PL10a, PL11]. This is not to belittle other research, but instead to highlight the lack of available databases and show that the dataset is far better than average in this particular field.

8.2.2 Algorithms

Both the state-of-the-art and proposed algorithm have been implemented using Matlab. Dissecting the two approaches gives a total of four different analyses. Each of the analysis creates a density map and extracts feature vectors in a similar fashions. The four different analyses are:

- Orientation Field Analysis (OFA).
- Minutia Distribution Analysis (MDA).
- Singular Point Density Analysis (SPD).
- Minutia Orientation Analysis (MOA).

The fusion of OFA and MDA constitute the state-of-the-art algorithm while the proposed method is constructed as a combination of the two remaining analyses, SPD and MOA.

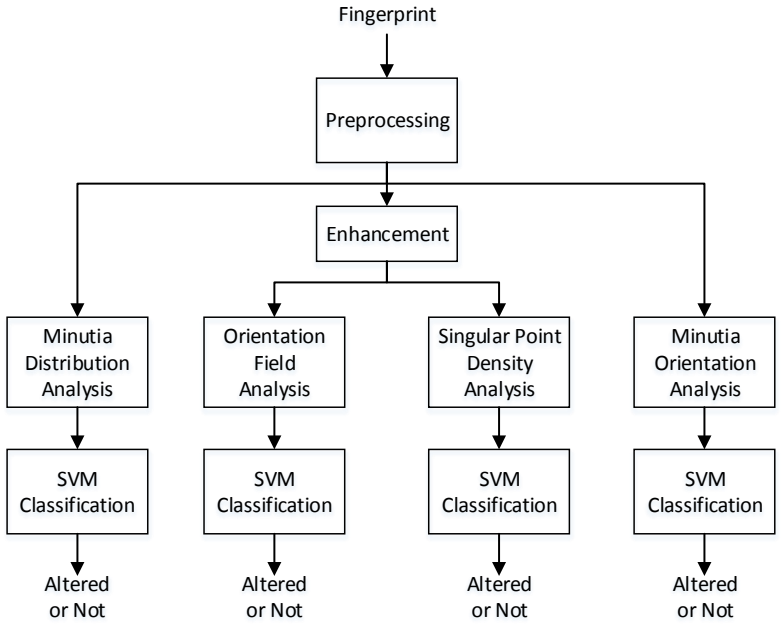

Figure 8.1: Tests were conducted on each analysis algorithm separately.

The four different analyses were tested separately. This was done by feeding the SVM with the 189-dimensional vector extracted from each analysis. The

preprocessing pipeline described in this thesis is used for all of the analyses. However, enhancement of the fingerprint image is not used on the two algorithms that analyse minutiae since it has its own preprocessing pipeline. Figure 8.1 shows the arrangement of the individual testing.

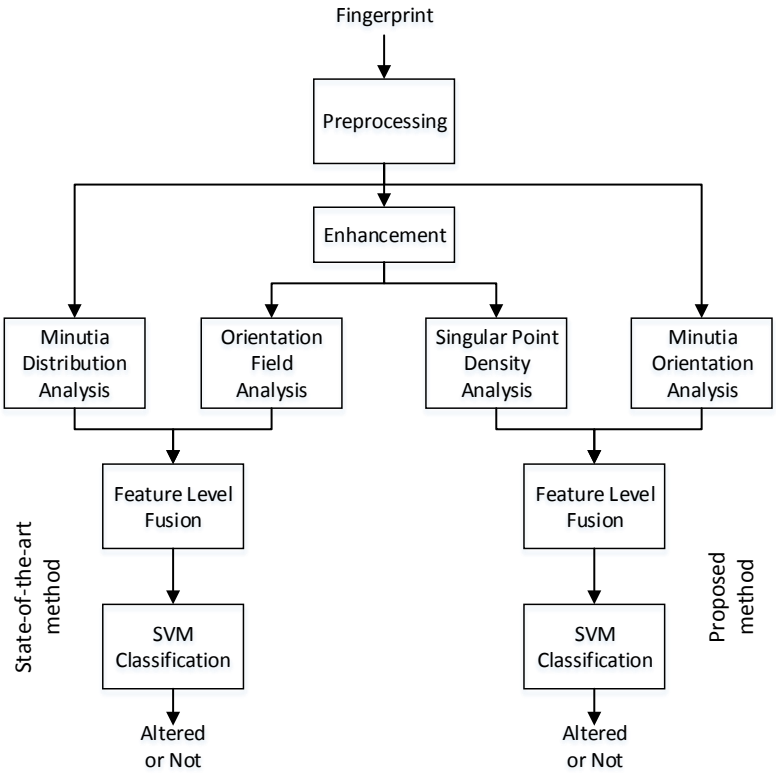

Figure 8.2: The state-of-the-art and proposed methods were tested separately.

Tests were conducted on the two methods, see Figure 8.2. An important step of the testing was to feed the same set of images to all tests so that comparisons can be done between the proposed and state-of-the-art method.

Additionally, a third method was proposed by combining the OFA from the state-of-the-art together with the SPD. Test results will show that this is a good combination since they are the two most reliable algorithms.

The testing currently contains a combination of three approaches each containing a pair of analyses. A majority voting scheme is also introduced which classifies a fingerprint as altered only if at least two of the methods give positive

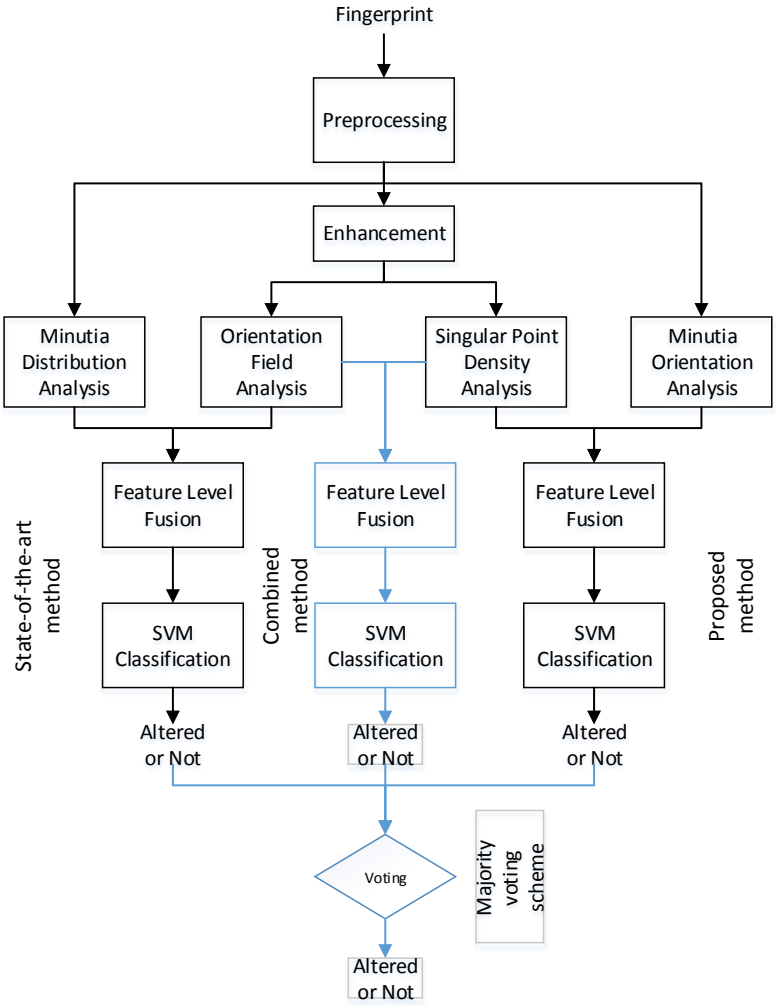

Figure 8.3: A combined test of the two most successful analyses was added. Additionally, a majority voting scheme was applied to vote on the results of all three methods.

classifications. The set up of the voting scheme can be seen in Figure 8.3.

8.3 Results

The experimental testing is performed using a SVM for classification. The *linear* kernel function was chosen as the best performing amongst the kernels tested. The SVM outputs binary (boolean) values: 1 when the system states that the presentation characteristic has been altered, and 0 otherwise.

For the purpose of cross-validation a total of ten test runs have been performed. The final test scores are based on the average scores of the test runs. For each test, the training and validation samples are randomly chosen from the available dataset. The randomisation algorithm used for preparing the samples is configured to select a common size and distribution between altered and unaltered for each test.

The size of the samples used for training and testing can be seen in Table 8.1. The testing set is larger due to the limited size of the database.

	Unaltered	Altered	Total
Training	94	35	129
Test	86	81	167
Total	180	116	296

Table 8.1: Average ratio between altered and unaltered fingerprint images used in each test. 296 fingerprint images were used by the test.

Yoon *et al* [YFJ12] use a more thorough 10-fold cross-validation which produces output results in the range $[0, 1]$. This gives additional options to fine-tune the results with regards to a desired proportion of TADR and FNADR. However, such a test is not possible given the available database size.

The final test results are given in Table 8.2. The full test results of each run can be found in Appendix A.

With a TADR of 91.9% and only 2.9% FNADR, the proposed method has a very similar detection rate to the existing method (91.7% TADR and 3.2% FNADR). However, combining the two most successful analyses from the two into one alteration detection method gives an even better performance with 94.6% TADR and 2.9% FNADR.

Using the proposed voting scheme that combines the three alteration detection algorithms (see Figure 8.3) gives the best results (95.1% TADR and 2.9% FNADR). The voting scheme requires at least two of the three methods to classify an image as altered in order to classify a fingerprint as altered.

Method	Analysis	TADR	FNADR
Existing	OFA	93.7%	3.2%
	MDA	77.5%	7.9%
	OFA/MDA	**91.7%**	**3.2%**
Proposed	SPD	92.0%	2.3%
	MOA	81.6%	5.5%
	SPD/MOA	**91.9%**	**2.9%**
Combined	OFA/SPD	94.6%	2.4%
Voting	OFA/MDA, SPD/MOA, OFA/SPD	95.1%	2.9%

Table 8.2: Test results. The existing algorithm (fusion of OFA and MDA) and the proposed algorithm (fusion of SPD and MOA) have very similar results. A fusion of OFA and SPD improves the result. The best results are achieved when combining all three fused methods using the voting scheme.

8.4 Evaluation

The proposed method is able to detect a high number of altered fingerprints, both obliterated and distorted. Not all altered fingerprints are detected by the algorithm, neither are all unaltered images classified as unaltered. The reason for this is the following:

- False non-altered detection. Some altered fingerprints have only a small area of alteration which can be hard to distinguish from a singular region. Also, some alterations don't provide significant minutiae or have very little change in the flow of the friction ridges along scarred regions.
- False altered detection. The main reason is poor image quality, especially around singular regions where the orientations have a high curvature.

The reproduction of the state-of-the-art method gives a firm basis on which to compare results. Extensive testing of the state-of-the-art method was performed by Yoon *et al* [YFJ12] on a much larger database from a government agency, publishing results of 70.2% TADR and 2.1% FNADR. Since the state-of-the-art method exhibited better performance on the current test database it might be an indication that the proposed method will perform slightly lower on a large scale database.

The proposed method has a fully comparable performance rate to the existing state-of-the-art algorithm based on the existing results. A list of images in Appendix B also testify to that fact that the algorithms are able to identify discrepancies in altered fingerprint images. The images have a higher density and greater distribution of high readings in altered fingerprints compared to unaltered.

The test results indicate that current alteration detection rates can be further improved by combining the SPD and OFA algorithms from the two different methods. Introducing the majority voting scheme will require a combination of all four analyses which complicates the detection algorithm and adds additional computation. However, the attractive results achieved by this method suggest a solution that delivers an increased detection rate with supreme accuracy that clearly outperforms the current state-of-the-art method.

In order to successfully evade identification by an AFIS, one is generally required to alter multiple fingertips. Most large-scale AFIS applications generally use a comparison score combined from all ten fingerprints. In such systems, five fingerprints are generally sufficient for reliable identification [YFJ12]. This could imply a system where at least five or six of the fingerprints should be classified as altered in order to raise an alarm, significantly minimising the chance for any false detections.

8.5 Summary

Experimental testing has been performed on a dataset composed from multiple sources. A reproduction of the state-of-the-art algorithm has enabled testing of both methods and additional combinations of both.

The proposed method has very similar results to the state-of-the-art method. It has also been shown that combining the most efficient analysis algorithm from each of the two methods, OFA from the existing and SPD from the proposed, improves the detection rate. The best results are achieved by using a voting scheme which votes on the results from the two methods along with results from the combined method.

Chapter 9

Directions for Future Works

This very brief chapter will identify some relevant directions for future works. Some of the items are already in process.

- Large scale testing. The experimental testing of the proposed method shows promising results. However, extensive tests on a larger scale need to be conducted in order to ensure the efficiency of the algorithms in detecting altered fingerprints.

  Based on the potential of the current results, the National Institute of Standards and Technology (NIST) in collaboration with the Department of Homeland Security (DHS) have agreed to run elaborate tests on the proposed method. The tests will be conducted in a similar fashion to the tests performed on the method proposed by Yoon *et al* [YFJ12]. It will test the proposed method, along with the current implementation of the state-of-the-art, and the proposed fusion of the two methods.

- Orientation entropy. Section 6.1.2 suggests that the orientation entropy has very distinct properties in altered fingerprints, as already observed by Tiribuzi *et al* [TPVR12]. Further study could be done to analyse the relationship and behaviour of the orientation entropy of altered and unaltered fingerprint images in order to possibly implement an alteration detection algorithm based on this technique.

- Standard quality measures. Fingerprint image quality assessment software such as NFIQ is used to evaluate the quality of a fingerprint image. The detection of fingerprint alteration has a very close relation to assessing the quality of a fingerprint image.

  Further work could be done to develop an approach to integrate alteration detection algorithms into already existent quality measures, such as introducing metrics on the probability that a fingerprint has been altered.

Chapter 10

Conclusion

The success of Automated Fingerprint Identification Systems (AFISs) has lead to an increased number of incidents where individuals alter their fingerprints in order to evade identification. Traditionally, fingerprint alteration was mainly seen in criminal cases, but today it is a common occurrence in non-criminal cases also. This is probably especially seen at border crossings where fingerprints are subject to comparison against a watch list.

This thesis has proposed a novel method for detecting altered fingerprints. The method is based on analyses of two different local characteristics of a fingerprint image. The first analysis identifies irregularities in the pixel-wise orientations which share similar characteristics to singular points. The second analysis compares minutia orientations covering a local, but larger area than the first analysis. A global density map is created in each of the analysis in order to identify the distribution of the analysed discrepancies.

Experimental results suggest that the method yields performance fully comparable to the current state-of-the-art method. Further improvements can be achieved by combining the most efficient analysis of the two methods, Orientation Field Analysis (OFA) and Singular Point Density Analysis (SPD). The best results were achieved by doing an elaborate analyses using all three methods (the proposed, state-of-the-art and the combined method) and additionally introducing a voting scheme to classify the fingerprint.

The promising results achieved in this study are attractive for further investigations. Especially, studies into the possibility of introducing alteration detection into standard quality measures of fingerprints which would improve AFISs and contribute to the fight against fraud.

Appendix A

Test Results

Analyses:

- Orientation Field Analysis (OFA)
- Minutia Distribution Analysis (MDA)
- Singular Point Density Analysis (SPD)
- Minutia Orientation Analysis (MOA)

The dataset contained a total of 296 images comprised by 116 altered and 180 unaltered fingerprint images. 10 test runs were performed on randomised training and validation samples.

	Unaltered	Altered	Total
Training	94	35	129
Test	86	81	167
Total	180	116	296

Table A.1: Average ratio between altered and unaltered fingerprint images used in each test. 296 fingerprint images were used by the test.

	OFA		MDA		Fusion	
Test #	TADR	FNADR	TADR	FNADR	TADR	FNADR
1	97.4%	4.7%	83.1%	5.8%	97.4%	5.8%
2	88.5%	3.5%	83.3%	15.3%	88.5%	2.4%
3	96.1%	3.4%	76.3%	3.4%	86.8%	3.4%
4	92.1%	1.1%	76.3%	6.9%	93.4%	1.1%
5	96.0%	8.0%	81.3%	14.8%	96.0%	6.8%
6	95.9%	3.3%	79.5%	13.3%	89.0%	6.7%
7	93.8%	1.2%	74.1%	3.7%	91.4%	1.2%
8	93.6%	3.5%	66.7%	2.4%	91.0%	2.4%
9	93.6%	3.5%	69.2%	2.4%	88.5%	2.4%
10	89.9%	0.0%	84.8%	10.7%	94.9%	0.0%
Avg	**93.7%**	**3.2%**	**77.5%**	**7.9%**	**91.7%**	**3.2%**

Table A.2: Test results of the state-of-the-art method. The *Fusion* method is the actual method which is the combination of the two analyses.

	SPD		MOA		Fusion	
Test #	TADR	FNADR	TADR	FNADR	TADR	FNADR
1	96.1%	1.2%	87.0%	4.7%	96.1%	2.4%
2	92.3%	3.5%	73.1%	7.1%	91.0%	2.4%
3	93.4%	4.6%	78.9%	8.0%	85.5%	2.3%
4	92.1%	1.1%	82.9%	5.7%	90.8%	4.6%
5	94.7%	4.5%	77.3%	5.7%	94.7%	2.3%
6	91.8%	3.3%	91.8%	8.9%	95.9%	7.8%
7	85.2%	0.0%	76.5%	1.2%	87.7%	1.2%
8	96.2%	3.5%	75.6%	3.5%	93.6%	2.4%
9	89.7%	0.0%	84.6%	4.8%	92.3%	2.4%
10	88.6%	2.3%	81.6%	5.5%	91.1%	1.2%
Avg	**92.0%**	**2.3%**	**81.6%**	**5.5%**	**91.9%**	**2.9%**

Table A.3: Test results of the proposed method. The *Fusion* method is the actual method which is the combination of the two analyses.

	OFA/SPD		Voting Scheme	
Test #	TADR	FNADR	TADR	FNADR
1	97.4%	3.5%	98.7%	3.5%
2	93.6%	1.2%	94.9%	1.2%
3	97.4%	3.4%	92.1%	3.4%
4	92.1%	0.0%	93.4%	1.1%
5	96.0%	6.8%	96.0%	6.8%
6	95.9%	3.3%	97.3%	6.7%
7	95.1%	0.0%	93.8%	0.0%
8	96.2%	3.5%	96.2%	3.5%
9	92.3%	2.4%	93.6%	2.4%
10	89.9%	0.0%	94.9%	0.0%
Avg	**94.6%**	**2.4%**	**95.1%**	**2.9%**

Table A.4: Test results of combining the OFA and SPD analyses, and the voting scheme using the state-of-the-art, proposed and OFA/SPD methods

Appendix B

Images

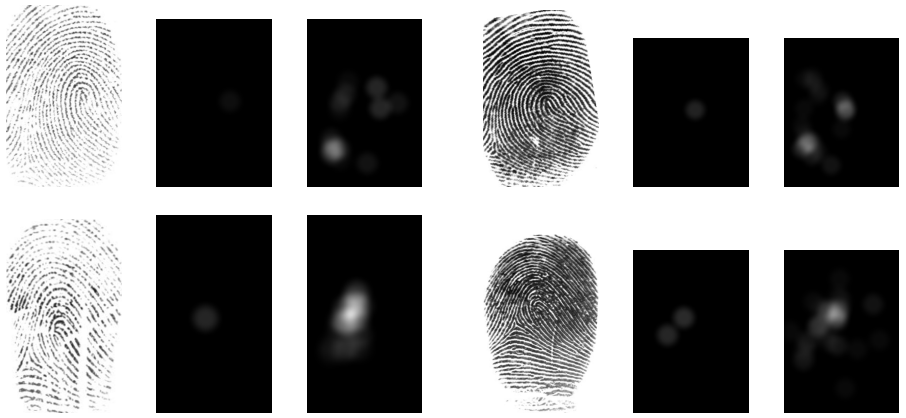

(a) Input **(b)** SPD **(c)** MDA **(d)** Input **(e)** SPD **(f)** MDA

Figure B.1: Images of final density maps of unaltered fingerprints.

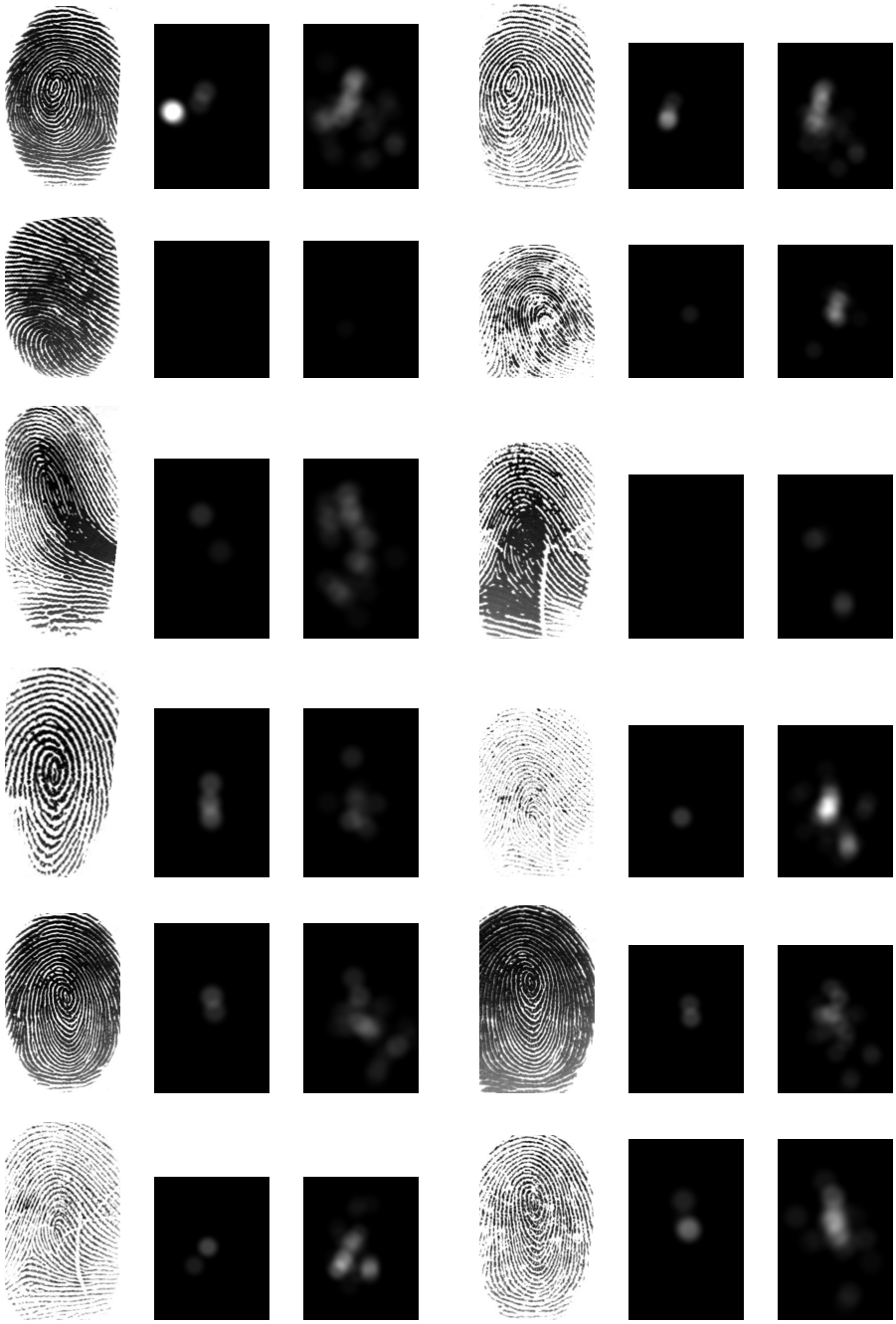

(a) Input (b) SPD (c) MDA (d) Input (e) SPD (f) MDA

Figure B.2: Images of final density maps of unaltered fingerprints.

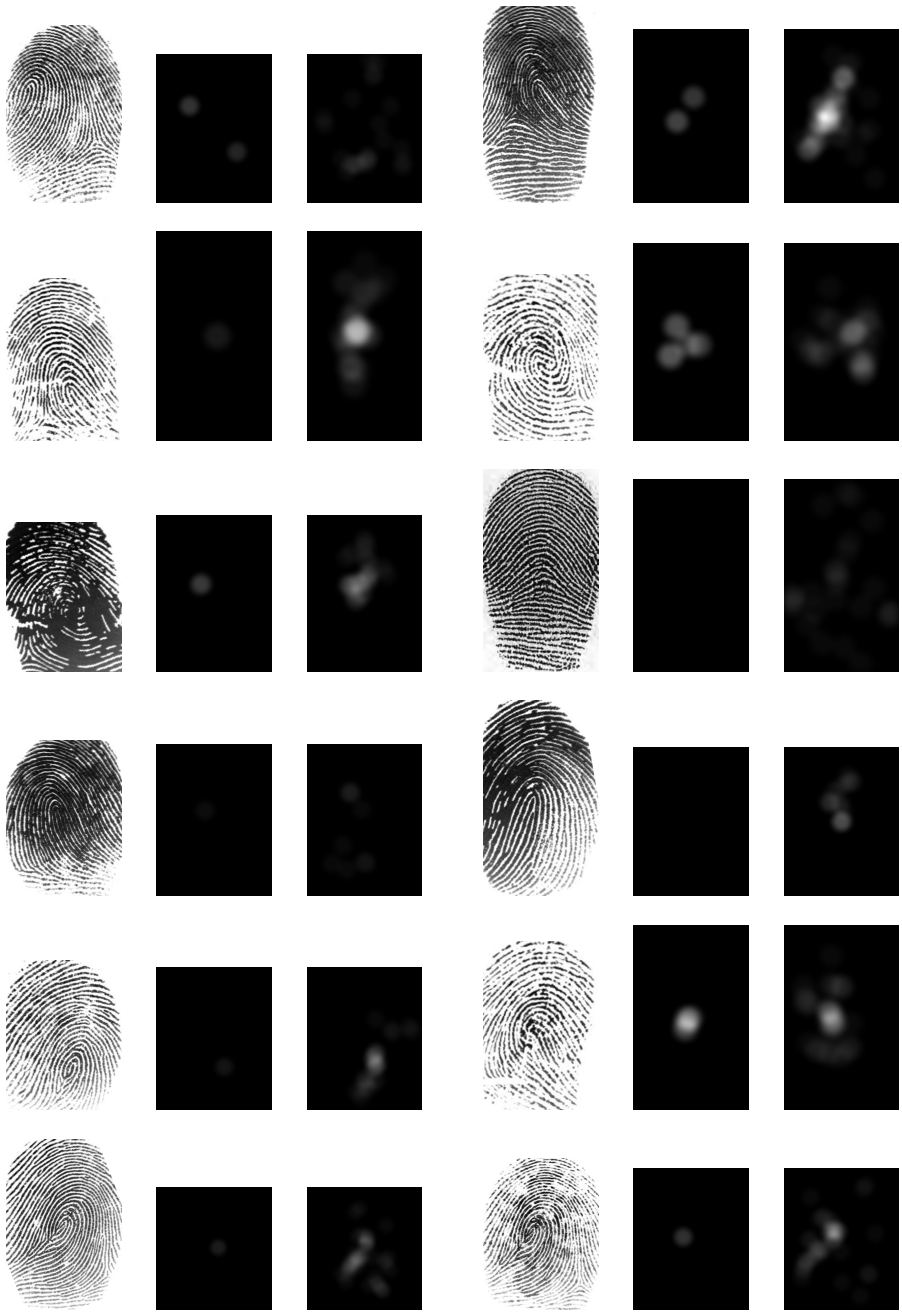

(a) Input **(b)** SPD **(c)** MDA **(d)** Input **(e)** SPD **(f)** MDA

Figure B.3: Images of final density maps of unaltered fingerprints.

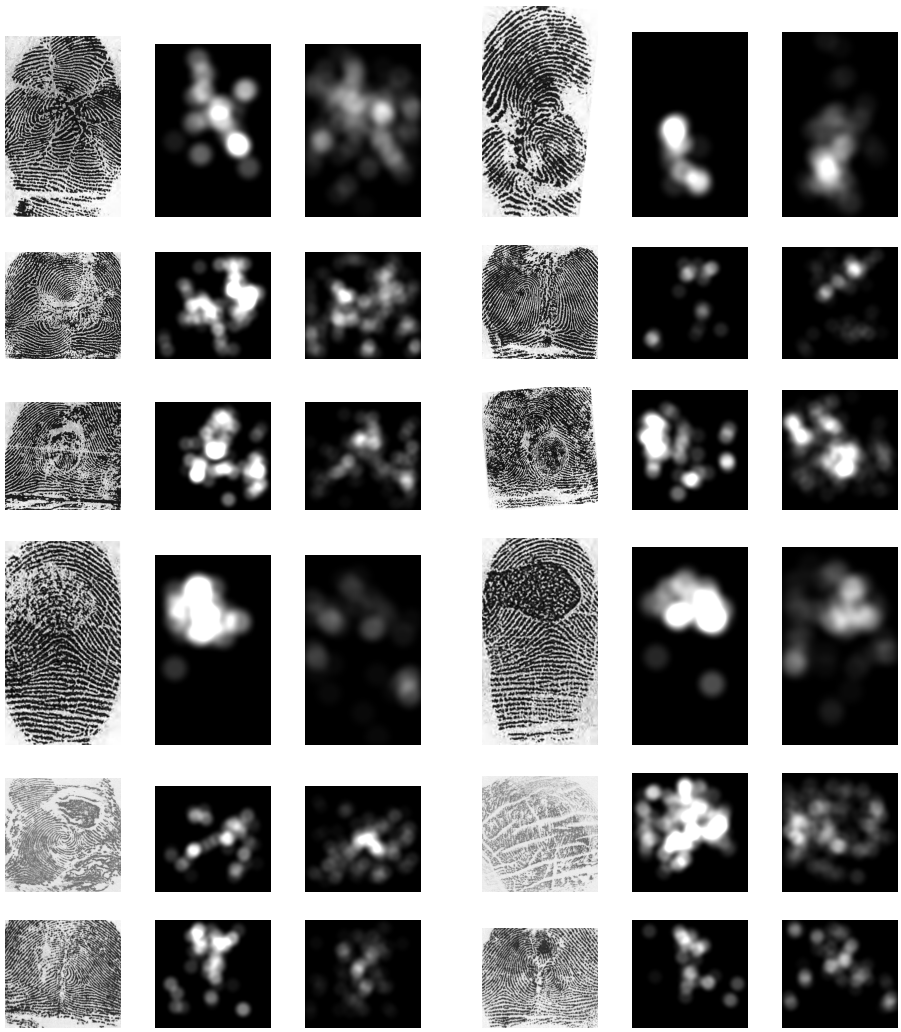

(a) Input (b) SPD (c) MDA (d) Input (e) SPD (f) MDA

Figure B.4: Images of final density maps of altered fingerprints.

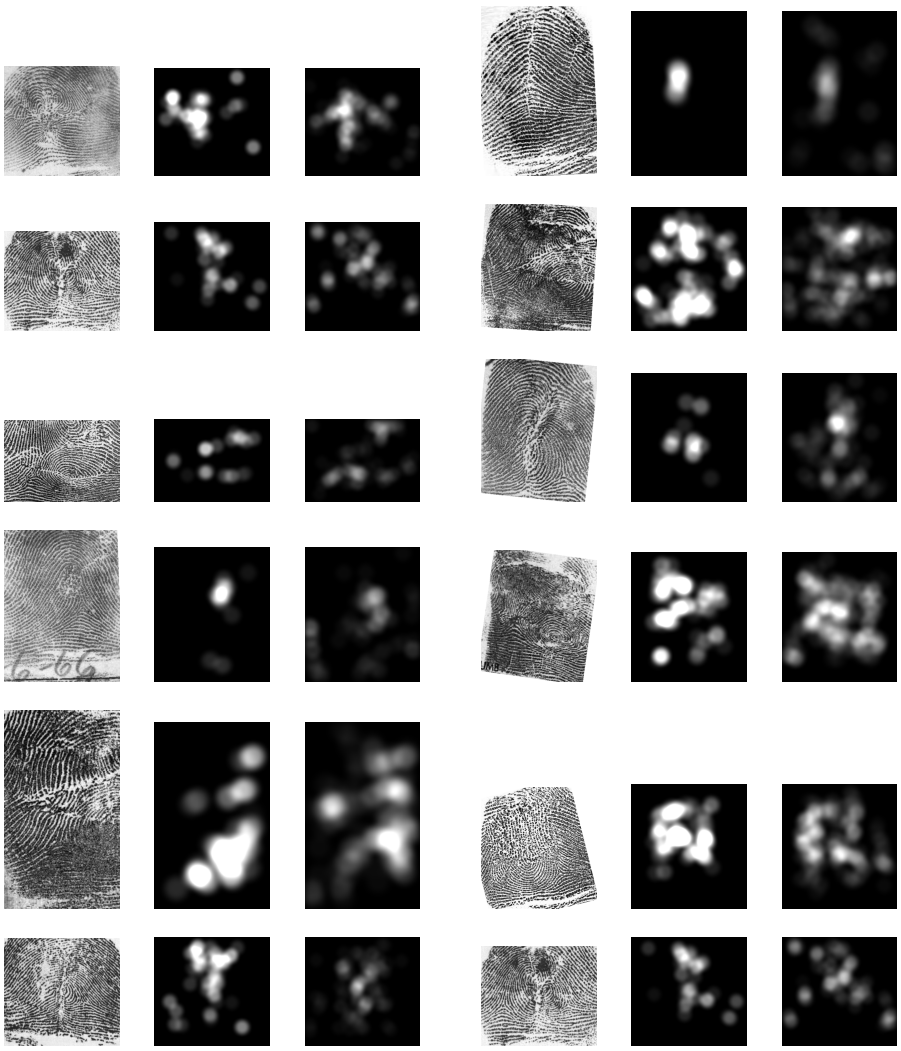

(a) Input (b) SPD (c) MDA (d) Input (e) SPD (f) MDA

Figure B.5: Images of final density maps of altered fingerprints.

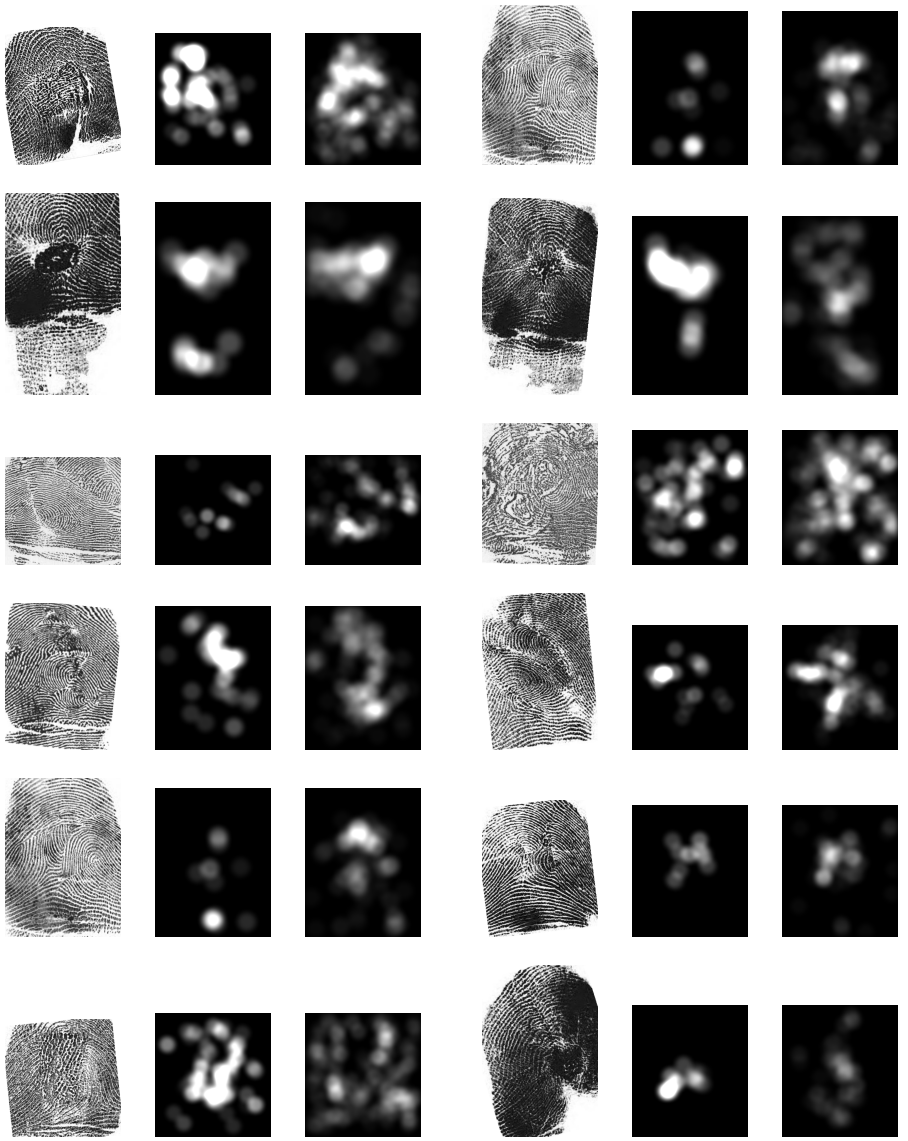

(a) Input **(b)** SPD **(c)** MDA **(d)** Input **(e)** SPD **(f)** MDA

Figure B.6: Images of final density maps of altered fingerprints.

Bibliography

[ACMM06] A. Antonelli, R. Cappelli, D. Maio, and D. Maltoni. Fake finger detection by skin distortion analysis. *Information Forensics and Security, IEEE Transactions on*, 1(3):360–373, 2006.

[AS09] Aditya Abhyankar and Stephanie Schuckers. Integrating a wavelet based perspiration liveness check with fingerprint recognition. *Pattern Recognition*, 42(3):452–464, 2009.

[BFMM05] Denis Baldisserra, Annalisa Franco, Dario Maio, and Davide Maltoni. Fake fingerprint detection by odor analysis. In David Zhang and AnilK. Jain, editors, *Advances in Biometrics*, volume 3832 of *Lecture Notes in Computer Science*, pages 265–272. Springer Berlin Heidelberg, 2005.

[BG01] Asker M. Bazen and Sabih H. Gerez. Extraction of singular points from directional fields of fingerprints. In *The 7th annual CTIT Workshop Mobile Communications in Perspective Workshop*, pages 41–44, Enschede, February 2001. Centre for Telematics and Information Technology.

[BG02] Asker M. Bazen and Sabih H. Gerez. Systematic methods for the computation of the directional fields and singular points of fingerprints. *IEEE Transactions on Pattern Analysis and Machine Intelligence*, 24(7):905–919, 2002. 060.02.

[BPL08] Jin Bo, Tang Hua Ping, and Xu Ming Lan. Fingerprint singular point detection algorithm by poincaré index. *WTOS*, 7(12):1453–1462, December 2008.

[Brn13] Fingerprint database. Alterations caused by diseases., March 2013. Faculty of Information Technology at Brno University of Technology and the research group STRaDe in collaboration with dermatologists from FN Olomouc.

[CCG05] Sharat S. Chikkerur, Alexander N. Cartwright, and Venu Govindaraju. Fingerprint image enhancement using STFT analysis. In *IN PROC. ICAPR*, pages 20–29, 2005.

[CMM+04] Maio Maltoni Cappelli, D. Maio, D. Maltoni, J. L. Wayman, and A. K. Jain. Fvc2004: Third fingerprint verification competition. In *in Proceedings of the First International Conference on Biometric Authentication*, pages 1–7, 2004.

[Com10] European Commission. Vis regulation, April 2010. http://europa.eu/legislation_summaries/justice_freedom_security/free_movement_of_persons_asylum_immigration/l14517_en.htm.

[Com12] European Commission. Visa information system - VIS, October 2012. http://ec.europa.eu/dgs/home-affairs/what-we-do/policies/borders-and-visas/visa-information-system/index_en.htm.

[CPL+11] Hongtao Chen, Liaojun Pang, Jimin Liang, Eryun Liu, and Jie Tian. Fingerprint singular point detection based on multiple-scale orientation entropy. *IEEE Signal Process. Lett.*, 18(11):679–682, 2011.

[Cum35] Harold Cummins. Attempts to alter and obliterate finger-prints. *Journal of Criminal Law and Criminology*, 25:982–991, 1935.

[DDU13] Michal Doležel, Martin Drahanský, and Jaroslav Urbánek. Einfluss von hauterkrankungen auf den biometrischen erkennungsprozess. *Datenschutz un Datensicherheit (DuD)*, Heft 6-2013:358–362, 2013.

[FJR09] Jianjiang Feng, Anil K. Jain, and Arun Ross. Fingerprint alteration. Technical Report MSU-CSE-09-30, Department of Computer Science, Michigan State University, East Lansing, Michigan, December 2009.

[GUC09] GUC100 Multisensor Fingerprint Database for in-House (Semipublic) Performance Test, January 2009. Gjøvik University College (GUC).

[GZ03] Jinwei Gu and Jie Zhou. A novel model for orientation field of fingerprints. In *IEEE Computer Society Conference on Computer Vision and Pattern Recognition*, pages 493–498, 2003.

[HC43] J. Edgar Hoover and Frederick L. Collins. The man without fingerprints. *Collier's Weekly*, page 16, January 1943.

[HHKA05] S. Hatami, R. Hosseini, Mahmoud Kamarei, and H. Ahmadi. Wavelet based fingerprint image enhancement. In *Circuits and Systems, 2005. ISCAS 2005. IEEE International Symposium on*, volume 5, pages 4610–4613, 2005.

[HLW03] Ching-Tang Hsieh, Eugene Lai, and You-Chuang Wang. An effective algorithm for fingerprint image enhancement based on wavelet transform. *Pattern Recognition*, 36(2):303 – 312, 2003.

[HUW+98] Yoshihiko Hamamoto, Shunji Uchimura, Masanori Watanabe, Tetsuya Yasuda, Yoshihiro Mitani, and Shingo Tomita. A gabor filter-based method for recognizing handwritten numerals. *Pattern Recognition*, 31(4):395–400, 1998.

[Int05] Method for fingerprint identification, january 2005. http://www.interpol.int/public/forensic/fingerprints/.

[ISO11] ISO/IEC. *ISO/IEC 19794-1:2011. Information Technology – Biometric data interchange formats – Part 1: Framework.* ISO/IEC, 2011.

[ISO12] ISO/IEC. *Text of 4th Working Draft 30107. Biometrics – Presentation attack detection.* ISO/IEC, 2012.

[JA07] J. Jeffers and A. Arakala. Fingerprint alignment for a minutiae-based fuzzy vault. In *Biometrics Symposium, 2007*, pages 1–6, 2007.

[Jai89] Anil K. Jain. *Fundamentals of digital image processing.* Prentice-Hall, Inc., Upper Saddle River, NJ, USA, 1989.

[JFNeb] Anil K. Jain, Jianjiang Feng, and Karthik Nandakumar. Fingerprint matching. *Computer*, 43(2):36–44, Feb.

[JKE07] Changlong Jin, Hakil Kim, and Stephen Elliott. Liveness detection of fingerprint based on band-selective fourier spectrum. In *Proceedings of the 10th international conference on Information security and cryptology*, ICISC'07, pages 168–179, Berlin, Heidelberg, 2007. Springer-Verlag.

[JPH99] A.K. Jain, S. Prabhakar, and L. Hong. A multichannel approach to fingerprint classification. *Pattern Analysis and Machine Intelligence, IEEE Transactions on*, 21(4):348–359, 1999.

[JPHP00] Anil K. Jain, Salil Prabhakar, Lin Hong, and Sharath Pankanti. Filterbank-based fingerprint matching. *IEEE Transactions on Image Processing*, 9:846–859, 2000.

[JPP01] Anil K. Jain, Salil Prabhakar, and Sharath Pankanti. Twin test: On discriminability of fingerprints. In *Proceedings of the Third International Conference on Audio- and Video-Based Biometric Person Authentication*, AVBPA '01, pages 211–216, London, UK, UK, 2001. Springer-Verlag.

[JPP02] Anil K. Jain, Salil Prabhakar, and Sharath Pankanti. On the similarity of identical twin fingerprints. *Pattern Recognition*, 35(11):2653–2663, 2002.

[JY12] Anil K. Jain and Soweon Yoon. Automatic detection of altered fingerprints. *IEEE Computer*, 45(1):79–82, 2012.

[KM95] T. Kamei and M. Mizoguchi. Image filter design for fingerprint enhancement. In *Computer Vision, 1995. Proceedings., International Symposium on*, pages 109–114, 1995.

[KMKA10] M. S. Khalil, D. Muhammad, M. K. Khan, and K. Alghathbar. Singular points detection using fingerprint orientation field reliability. *International Journal of Physical Sciences*, 5(4):352–357, 2010.

[KP02] Byung-Gyu Kim and Dong-Jo Park. Adaptive image normalisation based on block processing for enhancement of fingerprint image. *Electronics Letters*, 38(14):696–698, 2002.

[KT84] Masahiro Kawagoe and Akio Tojo. Fingerprint pattern classification. *Pattern Recogn.*, 17(3):295–303, June 1984.

[LHJ98a] Yifei Wan Lin Hong and Anil Jain. Fingerprint image enhancement: Algorithm and performance evaluation. *IEEE Transactions on Pattern Analysis and Machine Intelligence*, 20(8):777–789, 1998.

[LHJ98b] Yifei Wan Lin Hong and Anil Jain. Fingerprint image enhancement: Algorithm and performance evaluation. *IEEE Transactions on Pattern Analysis and Machine Intelligence*, 20(8):777–789, 1998.

[LJK05] Manhua Liu, Xudong Jiang, and Alex Chichung Kot. Fingerprint reference-point detection. *EURASIP J. Appl. Signal Process.*, 2005:498–509, January 2005.

[LJY02] Eyung Lim, Xudong Jiang, and Wei-Yun Yau. Fingerprint quality and validity analysis. In *Image Processing (ICIP), 2002 International Conference on*, volume 1, pages 469–472, 2002.

[Mai09] MailOnline. Calais migrants mutilate fingertips to hide true identity, July 2009. http://www.dailymail.co.uk/news/article-1201126/Calais-migrants-mutilate-fingertips-hide-true-identity.html.

[MIK+10] Johannes Merkle, Heinrich Ihmor, Ulrike Korte, Matthias Niesing, and Michael Schwaiger. Performance of the fuzzy vault for multiple fingerprints (extended version). *CoRR*, abs/1008.0807, 2010.

[MLBM11] I. S. Msiza, B. Leke-Betechuoh, and T. Malumedzha. Fingerprint re-alignment: a solution based on the true fingerprint center point. *Machine Learning and Computing (ICMLC 2011), IEEE International Conference on*, feb 2011.

[MMJP09] Davide Maltoni, Dario Maio, Anil K. Jain, and Salil Prabhakar. *Handbook of Fingerprint Recognition*. Springer Publishing Company, Incorporated, 2nd edition, 2009.

[New09] BBC News. "Fake fingerprint" chinese woman fools japan controls, December 2009. http://news.bbc.co.uk/2/hi/8400222.stm.

[NIS12] NIST. Development of NFIQ 2.0 - quality feature definitions. Technical report, June 2012.

[OXB12] M. A. Olsen, Haiyun Xu, and C. Busch. Gabor filters as candidate quality measure for NFIQ 2.0. In *Biometrics (ICB), 2012 5th IAPR International Conference on*, pages 158–163, 2012.

[PL10a] A. Petrovici and C. Lazar. Altered fingerprints analysis based on orientation field reliability. In *System Theory and Control, 2010 Proceedings of 14th International Conference on*, pages 385–391, 2010.

[PL10b] A. Petrovici and C. Lazar. Identifying fingerprint alteration using the reliability map of the orientation field. *The Annals of the Univeristy of Craiova. Series: Automation, Computers, Electronics and Mechatronics*, 7(34)(1):45–52, 2010.

[PL11] A. Petrovici and C. Lazar. Detection of altered fingerprints using a mahalanobis distance based classifier. In *Control Systems and Computer Science (CSCS18), 2011 Proceedings of 18th International Conference on*, pages 604–611, 2011.

[PL12] A. Petrovici and C. Lazar. Altered fingerprints analysis based on sift keypoints, 2012.

[Rav90] Rao A. Ravishankar. *A Taxonomy for Texture Description and Identification*. Springer-Verlag, New York, NY, 1990.

[REB10] Uday Rajanna, Ali Erol, and George Bebis. A comparative study on feature extraction for fingerprint classification and performance improvements using rank-level fusion. *Pattern Anal. Appl.*, 13(3):263–272, August 2010.

[Sam01] S.S. Samischenko. *Atlas of the Unusual Papilla Patterns / Atlas Neobychnykh Papilliarnykh Uzorov*. Urisprudentsiia, Moscow, 2001.

[Sha01] C. E. Shannon. A mathematical theory of communication. *SIGMOBILE Mob. Comput. Commun. Rev.*, 5(1):3–55, January 2001.

[SKK01] LinLin Shen, Alex ChiChung Kot, and Wai Mun Koo. Quality measures of fingerprint images. In *Proceedings of the Third International Conference on Audio- and Video-Based Biometric Person Authentication*, AVBPA '01, pages 266–271, London, UK, UK, 2001. Springer-Verlag.

[SLPD09] J. Scheibert, S. Leurent, A. Prevost, and G. Debrégeas. The role of fingerprints in the coding of tactile information probed with a biomimetic sensor, 2009.

[SMM94] B. G. Sherlock, D.M. Monro, and K. Millard. Fingerprint enhancement by directional fourier filtering. *Vision, Image and Signal Processing, IEE Proceedings* -, 141(2):87–94, 1994.

[SRBG11] Michael Schwaiger, Fares Rahmun, Oliver Bausinger, and Mathias Grell. Vispilot - towards european biometric visa border control. In Arslan Brömme and Christoph Busch, editors, *BIOSIG*, volume 191 of *LNI*, pages 3–10. GI, 2011.

[TPVR12] Michela Tiribuzi, Marco Pastorelli, Paolo Valigi, and Elisa Ricci. A multiple kernel learning framework for detecting altered fingerprints. In *Pattern Recognition (ICPR), 2012 21st International Conference on*, pages 3402–3405. IEEE, 2012.

[WCG94] C. I. Watson, G.T. Candela, and P.J. Grother. Comparison of fft fingerprint filtering methods for neural network classification. *NISTIR*, 5493, 1994.

[WE09] Peter H Warman and A Roland Ennos. Fingerprints are unlikely to increase the friction of primate fingerpads. *The Journal of Experimental Biology*, 212(Pt 13):2016–2022, 2009.

[Wer93] Kasey Wertheim. Altering prints, July 1993. http://onin.com/cgi-bin/fp/board-admin.cgi?action=quick&do=print&HTTP_REFERER=4/1494&postindex=415.

[Wer98] Kasey Wertheim. An extreme case of fingerprint mutilation. In *Journal of Forensic Identification*, volume 48, pages 466–477, 1998.

[WGT+] Craig I. Watson, Michael D. Garris, Elham Tabassi, Charles L. Wilson, R. Michael Mccabe, Stanley Janet, and Kenneth Ko. User's guide to NIST biometric image software (NBIS).

[WGTW12] C. Watson, M. Garris, C. Tabassi, and R. M. Wilson. NIST biometric image software, december 2012. http://www.nist.gov/itl/iad/ig/nbis.cfm.

[WM01] Andrew John Willis and L. Myers. A cost-effective fingerprint recognition system for use with low-quality prints and damaged fingertips. *Pattern Recognition*, 34(2):255–270, 2001.

[XYYP08] Shan Juan Xie, Ju Cheng Yang, Sook Yoon, and Dong-Sun Park. An optimal orientation certainty level approach for fingerprint quality estimation. In *Intelligent Information Technology Application, 2008. IITA '08. Second International Symposium on*, volume 3, pages 722–726, 2008.

[YFJ12] Soweon Yoon, Jianjiang Feng, and Anil K. Jain. Altered fingerprints: Analysis and detection. *IEEE Trans. Pattern Anal. Mach. Intell.*, 34(3):451–464, 2012.

[YFJR09] Soweon Yoon, Jianjiang Feng, Anil K. Jain, and Arun Ross. Automatic detection of altered fingerprints. ICPR, August 2009. Presentation.

[YLJF03] Jianwei Yang, Lifeng Liu, Tianzi Jiang, and Yong Fan. A modified gabor filter design method for fingerprint image enhancement. *Pattern Recogn. Lett.*, 24(12):1805–1817, August 2003.

[YMY07] Zhengmao Ye, Habib Mohamadian, and Yongmao Ye. Information measures for biometric identification via 2d discrete wavelet transform. In *CASE*, pages 835–840, 2007.

[YZJ12] Soweon Yoon, Qijun Zhao, and Anil K. Jain. On matching altered fingerprints. In *ICB'12*, pages 222–229, 2012.

[ZCG09] Jie Zhou, Fanglin Chen, and Jinwei Gu. A novel algorithm for detecting singular points from fingerprint images. *IEEE Transactions on Pattern Analysis and Machine Intelligence*, 31(7):1239–1250, 2009.

[ZWT02] Wei-Peng Zhang, Qing-Ren Wang, and Y.-Y. Tang. A wavelet-based method for fingerprint image enhancement. In *Machine Learning and Cybernetics, 2002. Proceedings. 2002 International Conference on*, volume 4, pages 1973–1977, 2002.

Acronyms

AFIS Automated Fingerprint Identification System. 1, 15, 21, 81, 87, 91, 92

APC Attack Presentation Characteristic. 2

CPL Center Point Location. 35

FADR False Altered Detection Rate. 79

FFT Fast Fourier Transform. 39, 40

FNADR False Non-Altered Detection Rate. 79, 80, 85, 86, 94, 95

MDA Minutia Distribution Analysis. 14, 23, 61, 82, 86, 93, 94, 97–102

MOA Minutia Orientation Analysis. 61, 73, 76, 82, 86, 93, 94

NBIS NIST Biometric Image Software. 15, 21, 32, 69

NFIQ NIST Fingerprint Image Quality. 9, 38, 90

OCL Orientation Certainty Level. 46, 47

OFA Orientation Field Analysis. 14, 20–23, 61, 82, 83, 86, 87, 91, 93–95

ROI Region Of Interest. 32, 33, 35, 37, 44, 51, 66, 72

SPD Singular Point Density Analysis. 45, 82, 83, 86, 87, 91, 93–95, 97–102

STFT Short Time Fourier Transform. 41

SVM Support Vector Machine. 14, 20, 23, 26–29, 82, 85, *Glossary:* SVM

TADR True Altered Detection Rate. 79, 80, 85, 86, 94, 95

TNADR True Non-Altered Detection Rate. 79

VIS Visa Information System. 1, 2

Glossary

core The core is defined as the *topmost point on the innermost recurving ridge-line of a fingerprint* [ISO11]. It can be seen as the point of maximum curvature of the concave ridges in the fingerprint image [JPHP00]. 35, 45

delta The delta is defined as a *point on a ridge at or nearest to the point of divergence of two typelines and located at or directly in front of the point of divergence* [ISO11]. Delta points are located at the center point where three different directions flows meet [KMKA10]. 45

friction ridges Flow-like patterns of ridges and valleys that exist on the surface of the palms and soles. On the fingers, the distinctive patterns formed by the friction ridges make up the fingerprints. 1

minutia Friction ridge characteristics that are used to individualize a fingerprint image. Minutia(e) are local discontinuities in the fingerprint pattern where friction ridges begin, terminate, or split into two or more ridges. 14, 21, 35, 61, 76

singular point Belongs to the set of features that can be detected at the global level. Singular points, called core and delta, act as control points around which the ridge lines are "wrapped" [MMJP09]. 13, 19, 27, 35, 45, 46, 51, 59, 66, 91

SVM A Support Vector Machine (SVM) performs classification by constructing a N-dimensional hyperplane that optimally separates the data into two categories. 109

visa shopping The practice of making further visa applications to other member states when a first application has been rejected. 2